

This is the peer reviewed version of the following article:

Substitution of sodium silicate with rice husk ash-NaOH solution in metakaolin based geopolymer cement concerning reduction in global warming / Kamseu, Elie; Beleuk à. Mounkam, L. M.; Cannio, Maria; Billong, Ndigui; Chaysuwan, Duangrudee; Melo, U. Chinje; Leonelli, Cristina. - In: JOURNAL OF CLEANER PRODUCTION. - ISSN 0959-6526. - 142:(2017), pp. 3050-3060. [10.1016/j.jclepro.2016.10.164]

Terms of use:

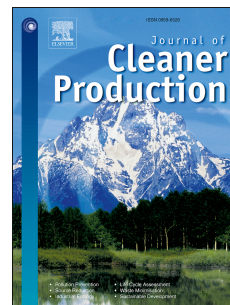
The terms and conditions for the reuse of this version of the manuscript are specified in the publishing policy. For all terms of use and more information see the publisher's website.

18/12/2025 18:12

Accepted Manuscript

Substitution of sodium silicate with rice husk ash-NaOH solution in metakaolin based geopolymer cement concerning reduction in global warming

E. Kamseu, L.M. Beleuk à Moungam, M. Cannio, Ndigui Billong, Duangrudee Chaysuwan, U. Chinje Melo, C. Leonelli



PII: S0959-6526(16)31795-4

DOI: [10.1016/j.jclepro.2016.10.164](https://doi.org/10.1016/j.jclepro.2016.10.164)

Reference: JCLP 8355

To appear in: *Journal of Cleaner Production*

Received Date: 30 March 2016

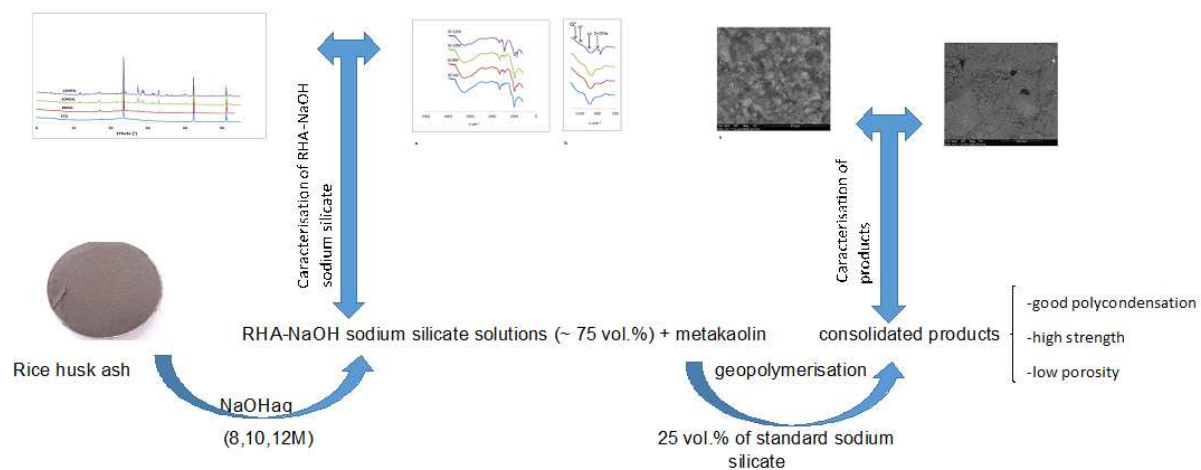
Revised Date: 8 October 2016

Accepted Date: 27 October 2016

Please cite this article as: Kamseu E, Beleuk à Moungam LM, Cannio M, Billong N, Chaysuwan D, Melo UC, Leonelli C, Substitution of sodium silicate with rice husk ash-NaOH solution in metakaolin based geopolymer cement concerning reduction in global warming, *Journal of Cleaner Production* (2016), doi: 10.1016/j.jclepro.2016.10.164.

This is a PDF file of an unedited manuscript that has been accepted for publication. As a service to our customers we are providing this early version of the manuscript. The manuscript will undergo copyediting, typesetting, and review of the resulting proof before it is published in its final form. Please note that during the production process errors may be discovered which could affect the content, and all legal disclaimers that apply to the journal pertain.

The paper's take away a message on a promising approach for the significant reduction of Global Warming Potential of geopolymers



Substitution of Sodium Silicate with Rice Husk Ash-NaOH solution in metakaolin based Geopolymer Cement concerning reduction in global warming

E. Kamseu^{1,2*}, L.M. Beleuk à MOUNGAM^{2*}, M. Cannio¹, Ndigui Billong², Duangrudee Chaysuwan³, U. Chinje Melo², C. Leonelli¹

¹Department of Engineering “Enzo Ferrari”, University of Modena and Reggio Emilia, Via Pietro Vivarelli 10, 41125 Modena, Italy.

²Local Materials Promotion Authority-MIPROMALO, P.O Box: 2396 Nkolbikok Yaoundé, Cameroon.

³Department of Materials Engineering, Faculty of Engineering, Kasetsart University, 50 Ngamwongwan Road, Chatuchak, Bangkok, 10900 Thailand.

Abstract: Rice husk ash (RHA), a by-product from the rice industry, was used as principal source of amorphous silica for the production of sodium silicate solution (MR ~ 3) used for the replacement of standard commercial sodium silicate in the mix-design of metakaolin based geopolymer composites. Three initial concentrations of NaOH were considered (8, 10 and 12M) with the aim to investigate on the optimum dissolution and formation of silica oligomers capable to act as binder during the geopolymerization. Results (FT-IR and XRD) showed that RHA-NaOH sodium silicate solutions have characteristics similar to that of standard commercial sodium silicate and the residual carbonates present in the viscous pastes can be monitored during the preparation of geopolymers using the mix-design. Combined 25 vol.% standard sodium silicate solution with ~ 75 vol.% of RHA-NaOH based sodium silicate solution conducted to good polycondensation, densification, high flexural strength (~ 8 MPa) and low porosity similar to that of the standard matrix of metakaolin based composites. The new approach is found promising for the significant reduction of the Global Warming Potential of Geopolymers.

Keywords: Rice husk ash, sodium silicate, geopolymer, sustainable, Global Warming Potential.

*Corresponding Authors: Kamseu Elie (kamseuelie2001@yahoo.fr); Beleuk à MOUNGAM Lynn Myllyam (belynn20@yahoo.fr).

1. Introduction

The geopolymerization mechanism is founded into the ability of Al and Si oligomers liberated in high alkaline solution to polymerize into $\text{Na(K)-(Al)}_n\text{-(Si)}_m\text{-H}$ with $1.5 < m/n < 3$. In this range of formulations, soluble silica and alumina will develop structural 3D units. To activate the amorphous to semi-crystalline solid precursors to form aluminosilicate oligomers, the alkaline solution is generally necessary. The alkaline solution is formed from (i) a high hydroxide solution with concentration $> 5\text{M}$ capable to dissolve the amorphous fraction of the solid powders in solution; (ii) a sodium/potassium silicate solution that provide appropriate amount of soluble silica prompt to tackle Al oligomers and form polysialates (Davidovits, 2008). Amongst the two solutions, the sodium/potassium silicate is actually that with the higher concern regarding the effective and efficient sustainability of geopolymer (Habert et al., 2011). However as new technology to be implemented and particularly for the developing countries and the challenge of wastes management, sustainable and cleaner geopolymers locally sourced and produced using renewable resources, with negligible transport costs and environmental impact, with low energy required in the manufacturing process is targeted. In this study we are proposing the partial substitution of the sodium silicate solution with amorphous Rice Husk Ash (RHA) combined NaOH in solution. Solutions of sodium silicate with $\text{SiO}_2/\text{Na}_2\text{O} \sim 3$ have shown a relatively complex structure, containing a fraction of dissolved low molecules weight silica species as well as a relatively high amount of larger clusters dominated by cyclic or cage structures. It should be added the presence of larger colloidal particles, several tens of nm in radius. The fraction of soluble silica and small oligomers species decreases when increasing the $\text{SiO}_2:\text{Na}_2\text{O}$ ratio until a ratio of 4 is reached. It is in the range of $\text{SiO}_2:\text{Na}_2\text{O}$ of 2-3 that good equilibrium is achieved between the fraction of monomers and that of clusters in the way to ensure the optimum polymerization/polycondensation during geopolymerization. Authors (Nordstrom et al., 2013; Nordstrom et al., 2011) analysed a serie of silicate solutions with SiO_2 concentrations from 12 to 28 wt.% and a molar ratio varying between 0.05 and 4.0. They showed that for a solution of 27.2 wt.% and a $\text{SiO}_2:\text{Na}_2\text{O}$ ratio of 3.3, 35 wt.% of silica is fully polymerized. Polymerization leads to more branching and eventually to predominantly three dimensional cage-like species at ratios ~ 3 (Svensson et al., 1986).

The production of sodium silicate involves the calcination of sodium carbonate (Na_2CO_3) and quartz (SiO_2) at temperatures between 1400 and 1500°C, producing large amounts of CO_2 as a secondary product (Turner and Collins, 2013; Rodriguez et al., 2013). The need of high temperature to process substantially increases the embodied energy of silicate-activated binders, reducing significantly their sustainability. The project to use RHA to replace soluble silica in the alkaline

solution for geopolymerization firstly appears as solution for the recycling of agricultural/natural wastes. Secondly their effective introduction into the geopolymer synthesis will significantly reduce the Global Warming Potential (GWP) of the process and products. - their work on carbon dioxide equivalent emissions making a comparison between geopolymers and Ordinary Portland Cement (OPC) concretes, Turner and Collins (2013) indicated that the major components responsible for the CO₂ emission are sodium silicate and curing with sodium silicate accounting for ~ 50 vol.%. Their work agreed with the preoccupation of Habert et al. (2011). The RHA-NaOH system is viewed as viable and cleaner solution to optimize the sustainability of geopolymer binders and concretes. McLellan et al. (2011) and Heath et al. (2014) agreed on the possible reduction up to 40-44 vol.% of GWP with geopolymer science and technology at the place of OPC. They generally make reserve on the secondary costs linked to production and transportation.

2. Rice Husk Ash and project design

The world production of rice husk ash is about 20 million tons (Nagrle et al., 2012). Prior to Metha (1992), RHA was usually produced using uncontrolled combustion and the ash produced was generally crystalline and had poor pozzolanic properties. One of the first studies (Metha, 1973) on RHA reactivity investigated the effects of pyroprocessing parameters on the pozzolanic reactivity of RHA. RHA treated under the ASTM standard C618-94a will produce amorphous silica with 90-96% of SiO₂. RHA used in cementitious binders presents particles around 8.3 µm with specific gravity of 2.05, nitrogen absorption of 20.6 m²/g, water requirement of 104% and pozzolanic activity index of 99%. The microsilica can be a source for preparing advanced materials like SiC, Si₃N₄, elemental Si and Mg (Chandrasekhar et al., 2003). Due to the high pozzolanic activity, the rice husk ash silica also finds application in high strength concrete and possibly as filler in polymers (Chandrasekhar et al., 2003). The activity of RHA is essentially linked to the amorphous structure of the SiO₂ that allows their chemical transformation. It is generally agreed that amorphous silica will be obtained between 500 and 700°C. The silica in RHA is X-ray amorphous, ultrafine in size, highly porous and chemically reactive. We wish to exploit the solubility of amorphous silica from RHA in high alkaline solution (pore solution similar to that of geopolymerization context) to prepare sustainable activator that is more environmentally clean.

3. Materials and Experimental methods

3.1 Materials

Rice husk ash (RHA) were from a rice mill in Angthong province in Thailand. The ash was collected as produced into the waste treatment deposit and ground to fine powder lower than 45 μm . The metakaolin was used as a solid precursor for the geopolymer binders because of its high reactivity, fine particle size and Si/Al appropriate for the development of N-A-S-H type geopolymer gels (Kamseu et al., 2014). Metakaolin powder is characterized by a very high surface area per unit volume because it is composed of plate-like shape particles with reactive sites on the surface (Kamseu et al., 2014). The metakaolin (MK) was prepared using high quality of white kaolin ($5.4\text{SiO}_2 \cdot 4\text{Al}_2\text{O}_3$) commonly used for glaze in ceramic tile industry (BAL-CO S.p.A, Sassuolo, Italy). Kaolin was calcined at 700°C for 4h to decomposed phyllosilicates and then it was pulverized reaching grain size below 60 μm . Mineralogical analysis of MK shows minor crystalline impurities identified as alpha-quartz (ICDD # 89-8934). Physical characteristics of metakaolin as well as those of fines are reported in Table 1.

The NaOH solution was prepared by dissolving laboratory grade granules (96 wt.%, Sigma Aldrich, Italy) into distilled water to have 8, 10 and 12M concentrations. The sodium silicate solution ($\text{SiO}_2/\text{Na}_2\text{O} = 3.00$ molar ratio; $\text{SiO}_2 = 26.50$ wt.%, $\text{Na}_2\text{O} = 8.70$ wt.% and $\text{pH} = 11.7$) with bulk density of 1.34 at 20°C was provided by Ingessil, Verona, Italy.

3.2 Preparation of RHA-NaOH sodium silicate solution and Metakaolin based geopolymer composites

Appropriate amount of fine powder of RHA (particle size < 45 μm) is weighed and introduced in NaOH solution of 8, 10 and 12M. The mix is ball-milled in a porcelain jar using a rapid Mill (1200 rpm) for 40 min. The homogeneous liquid is stored for a minimum of 24 h before the use. A standard formulation of metakaolin based geopolymer cement was developed. Sodium hydroxide (8M) and sodium silicate solutions are mixed in the 1:1 volume ratio and used to activate metakaolin powder. Sand is added in the metakaolin:sand ratio of 1:2. Finally, the solid/liquid ratio of the system was ~ 1.7 . For the sodium silicate solutions prepared with initial NaOH solution of 10 and 12M, the alkaline solution is adjusted with distilled water prior to the mix with the solid precursor. The highly viscous pastes obtained was poured into 140 mm x 15 mm x 15 mm silicon molds.

The three sodium silicate solutions prepared allowed to have 8M100, 10M100 and 12M100: formulations of metakaolin based geopolymers with 100 vol.% of sodium silicate made from RHA-NaOH systems. Successively, 8M75, 8M50 and 8M25 were prepared with sodium silicate solution (RHA-NaOH, 8M) replaced progressively with 25, 50 and 75 vol.% of standard commercial (MR = 3.00) sodium silicate solution. Similar substitution was made with 10 and 12M sodium silicate solutions to have 10M75, 12M75, 10M50, 12M50, 10M25 and 12M25. The geopolymers pastes obtained were stored into plastic for 24 h to avoid any contact with air. After 24 h, the curing of the specimens continued in a conditioned oven with 80% of relative humidity and temperature of 30°C for 72 h still in plastic. The specimens are then stored at ambient temperature ($21 \pm 2^\circ\text{C}$; RH ~ 54%) for more than 28 days before characterization.

3.3 Characterization of the inorganic polymer cements and composites

Mineralogical analysis of the inorganic polymer cements and composites were carried out with an X-ray powder diffractometer, XRD, (PW3710, Phillips) $\text{CuK}\alpha$, Ni-filtered radiation (the wavelength was 1.54184\AA). The radiation was generated at 40 mA and 40 kV. The analysis was performed on fine grains of ground samples. Specimens were step-scanned as random powder from 5 to 70°C , 2 theta steps were integrated at the rate of 2 s per step.

Fourier transformed infrared spectroscopy, FT-IR, (Avatar 330 FTIR, Thermo Nicolet) was performed on each sample analyzing fine powder of ground specimens ($\phi < 80\text{ }\mu\text{m}$) collected from pieces of the mechanical test cured at 28 days. A minimum of 32 scans between 4000 and 500 cm^{-1} were averaged for each spectrum at intervals of 1 cm^{-1} .

An Autopore IV 9500, 33000 psia (228 MPa) Mercury Intrusion Porosimeter (MIP) covering the pore diameter range from approximately 360 to $0.005\text{ }\mu\text{m}$ having two low-pressure ports and one high-pressure chamber was used for the pores analysis. Pieces were prepared from the bulk of each sample with specimens of $\sim 1\text{ cm}^3$ of volume for the MIP.

3.4 Three point flexural strength and Young Modulus

Specimens (10 for each composition) with nominal size of $10 + 0.10\text{ mm}$ in width, $10 + 0.10\text{ mm}$ thick and a length of 140 mm were used. The specimens were placed in an appropriate sample holder and loaded in an universal testing machine (type MTS 810, USA) with a cross-head speed of 3 mm/min until failure. The span between the two platens of the sample holder was 40 mm. Supports and loading piston were steel knife edges; rounded to a radius of 1 mm. Load was applied at the midpoint of the specimens. The strength is given by the equation (1):

$$\sigma = \frac{3 F l}{2 b h^2} \quad (1)$$

Where σ is the maximum center tensile stress (MPa), F maximum load at fracture (N), l the distance between the supports (mm), b the width and h the thickness of the specimen (mm). The Three-point bending strength tests were performed according to the standard test method for flexural strength of advanced ceramics at ambient temperature: ASTM C1161-02c.

The microstructure of the inorganic polymer cement and composites specimens was studied using an Environmental Scanning Electron Microscope (ESEM, Model Quanta 200) at low vacuum. Both fractured pieces from mechanical testing, and etched polished specimens were used for microstructural investigations. Polished samples were mounted in resin and polished using 1 μ m diamond paste for final polishing. To ensure the conduction of electron and prevent charging during the ESEM analysis, specimens were coated with 10 nm thick gold layer to allow a better resolution during the micrographs collection. The ESEM was equipped with an Oxford Instruments Energy Dispersive Spectrometer (EDS) for the microanalysis facilitating the investigation of phase distribution in the matrices.

4. Results

4.1 Silica condensation in standard and RHA-based sodium silicate

Both X-ray diffraction and FT-IR spectroscopy were used to elucidate the silica condensation in the RHA-based sodium silicate in comparison to the standard one. Fig. 1 and 2 show the XRD and FT-IR patterns of the solutions where RHA was activated/dissociated with 8, 10 and 12M solution of NaOH. The standard sodium silicate solution with molar ratio of 3 used as reference showed XRD diffuse peak at $2\theta = 28.71^\circ$, characteristic of disordered aluminosilica structures (Fig. 1). Broad diffuse halo in XRD patterns corresponds to three-dimensional networks for low angle compositions ($2\theta < 30^\circ$) while the high angle compositions ($2\theta > 30^\circ$) is generally attributed to low molecular weight silicate (dimer, monomer) (White et al., 2011; Bignozzi et al., 2013). Fig. 1 confirms that larger fraction of silicate into the sodium silicate solution prepared are essentially in form of clusters, colloidal gels, etc with 3D network structure. It should be noted that the position of the halo that is at 28.71° a little far from $25-27^\circ$ that generally characterize 3D structures of amorphous aluminosilicates come from the fact that although clusters and colloidal structures, the sodium silicate in this range of concentration present also an amount of 2D silica in form of monomers and dimers. The additional peaks observed are from carbonates that crystallized during the curing/solidification at ambient temperature of as prepared solutions. From the Fig. 2, it is

observed that all the characteristic peaks of standard sodium silicate solution are represented in all the three samples of RHA-based sodium silicate. The OH vibration band (νOH) of water is observed at 3207 cm^{-1} for the standard sodium silicate. It appeared at 3162 cm^{-1} for the RHA-based sodium silicate 8M. The values increased to 3174 cm^{-1} and 3195 cm^{-1} respectively for those at with 10M and 12M NaOH. The binding of water molecules ($\delta\text{H}_2\text{O}$) is identified at 1616 cm^{-1} in standard sodium silicate solution and that activated with 12M NaOH. The peaks is observed at 1631 cm^{-1} for the solution 8M and 1623 cm^{-1} for that with 10M NaOH. It is observed that by increasing the concentration of NaOH, the intensity of the peak at 1616 cm^{-1} increases as the shoulder at 3207 cm^{-1} . The increase of NaOH concentration also increases the significance of the peak at 1400 cm^{-1} which is that of carbonate compounds. The mean peak of sodium silicate solution that characterizes the asymmetric stretching ($\nu_{\text{as}}\text{Si-O-Si}$) of Si-O-Si bonds at 962 cm^{-1} for the standard sodium silicate solution appeared at 950 cm^{-1} , 946 cm^{-1} , 943 cm^{-1} respectively for the solutions with 8, 10 and 12M (Fig. 2). The results agreed with what has been discussed by Tongnonvi et al. (2012a and b). In fact in relative high silica concentration and pH above 11, stable solution of sodium silicate is formed. The concentration of clusters (Q^3 and Q^4) in solution decrease rapidly as the pH increase between 11 and 14. In the meantime the concentration of the Q^2 shifts progressively to lower values of wavenumber. Nordstrom et al. (2011) demonstrated that in $\text{SiO}_2\text{:Na}_2\text{O}$ molar ratios between 3.3 and 8.9, the intensity of the peak at 1000 cm^{-1} decreases while that at 1100 cm^{-1} increases. In the sodium silicate solution with the $\text{SiO}_2\text{:Na}_2\text{O}$ molar ratio of 3, most of the silica is present as small clusters with a radius of 0.7 nm and 11-13 wt.% of the silica present are even smaller such as monomers or smaller oligomeric species. Very small fraction of the silica is detected as larger colloidal particles in the size $\geq 30\text{ nm}$.

4.2 Characterization of the interaction between the NaOH-RHA based sodium silicate and the geopolymer pastes.

The FT-IR spectra of the geopolymer matrices with various fraction of RHA -NaOH sodium silicate presents the common features of the metakaolin based geopolymer composites with the bands at 3200 cm^{-1} which is that of OH vibration (νOH), the binding of water molecules ($\delta\text{H}_2\text{O}$) at 1640 cm^{-1} as in the FT-IR spectra of silicates (Fig. 2). The spectra that are directly affected by the $\text{SiO}_2\text{:Na}_2\text{O}$ ratio and those sensitive to the variation of pH, mainly the asymmetric stretching ($\nu_{\text{as}}\text{Si-O-Si}$) of Si-O-Si bond at $\sim 1000\text{ cm}^{-1}$ (Tognonvi et al., 2012b; White et al., 2011), the deformation ($\delta\text{Si-OH}$) of Si-OH at 870 cm^{-1} and the bands at 1100 cm^{-1} , 796 cm^{-1} , 775 cm^{-1} and 694 cm^{-1} assigned to quartz from the silica sand of the geopolymer composites were particularly investigated. From Fig. 3a, it is observed that the position of the principal band of the asymmetric stretching that is known to be a

characteristic of H-N-A-S phases is at 964 cm^{-1} for the standard geopolymer and 100% NaOH-RHA based sodium silicate at 8M. By increasing the fraction of the standard sodium silicate, the position of the band shifts to high value of wavenumber. This was verified also for the 10M concentration (Fig.3b) and 12M (Fig. 3c). The variations from Fig. 3a to Fig. 3c are indicative on the level of chemical interaction between the solid precursor and the RHA-NaOH based sodium silicate solution. The shift from the specimens at 8M and those at 10M is linked to the difference in the level of dissolution of the amorphous silica at different concentration. In the case of 10M, more reactive Si-OH groups are available due to the prior attack of the amorphous silica by OH-hydroxide during the dissolution in the preparation of the RHA-NaOH sodium silicate. Higher wavenumber is characteristic of the reduction of Si-O-Si angle and the increase in the concentration of three dimensional siloxane networks (Brew and Glasser, 2005; Gerschel, 1995). The combination of the standard sodium silicate and RHA-NaOH based conducted to a shift of the wavenumber to high value up to 75 vol.% and all the specimens with RHA-NaOH silicate seen the wavenumber of Q^2 decrease to low values (Fig. 3d). This suggest that, the mechanism of geopolymerization in this case is more complex including not only the level of dissolution of the amorphous silica from RHA. Obviously it can be suggested the action of the finer particles of silica from the standard sodium silicate and coarse ones from RHA-NaOH. Increasing NaOH concentration, the amount of fine particles increases in relation with the extend of dissolution improving the formation of 3D network. The amount of the carbonates included into the matrix of geopolymers (Fig. 3) correlates with the hypothesis of the synergetic action of the two soluble silica solutions which surely have compatible granulometry to enhance the polymerization of the matrices. Between 25 and 50 vol.% of RHA, the carbonates content into the samples is stable under 6 wt%. The peak of the halo is slightly shifted from 28.71 for the standard sodium silicate to 27.63 and 27.61 for the specimens with 8 (Fig. 4a), 10 (Fig. 4b) and 12M (Fig. 4c) respectively. This confirm the high rate of polymerization within the geopolymer matrices compared to the sodium silicate. It is difficult with the XRD patterns dominated with the quartz peaks to appropriately identify the presence of carbonates into the matrices. The low content of these carbonates did not allow clear evidence in FT-IR (Fig. 3). However appropriate chemical geopolymer process conducted to a clear decrease of carbonate with the increase of the soluble silica from standard sodium silicate. Evidently from the intrinsic characteristics of the silicate solution with more fine particles prompt to react in solution with respect to the silica from RHA-NaOH which the delay may be at the origin of the formation of carbonates.

4.3 Cumulative pore volume, pore size distribution, water absorption-desorption

Fig. 5 presents the cumulative pore volume of the formulations of geopolymers with RHA-NaOH sodium silicate prepared with 8M (Fig. 5a), 10M (Fig. 5b) and 12M (Fig. 5c). In general, the cumulative pore volume decreases with the increase of NaOH concentration, and with the fraction of the standard sodium silicate. From the Fig. 5a, specimens prepared with RHA-NaOH 8M presents cumulative pore volume of 0.267 (100% RHA-NaOH based sodium silicate), 0.196 (75% RHA-NaOH based sodium silicate), 0.162 (50% RHA-NaOH based sodium silicate) and 0.181 mL/g (25% RHA-NaOH based sodium silicate). The series with RHA-NaOH 10M presents values of cumulative pore volume of 0.198, 0.184, 0.177 and 0.171 mL/g when 100, 75, 50 and 25% of prepared RHA-NaOH sodium silicate is used. The cumulative pore volume of specimens with RHA-NaOH 12M do not change significantly from those with 10M being 0.206, 0.185, 0.182 and 0.173 respectively. The values of the cumulative pore volume of Fig. 5 are similar to those generally described with the metakaolin based inorganic polymer cement (Kamseu et al., 2014; Kamseu et al., 2013; Okada et al., 2011). The pores in those samples are divided into two groups: (i) those with size $\geq 0.24 \mu\text{m}$ and the finer with size $< 0.24 \mu\text{m}$. In both cases, the volume decrease with the concentration of NaOH. The average volume of the pores with $\phi \geq 0.24 \mu\text{m}$ are $\sim 38\%$ in 8M series, 35% in 10M series and 25% in 12M series. The significant reduction in cumulative pore volume is achieved with the serie 8M where the addition of the standard sodium silicate affect the cumulative pore volume in a significant manner. It should be noted that as from 25% of standard sodium silicate added into formulations, there is no more significant difference between the cumulative pore volumes of these formulations with RHA-NaOH from 8 to 12M and in most cases this slight difference could be explained with errors bars or sampling.

Fig. 6 shows the significant reduction of the pores with a shift of their peaks to lower values. From $0.229 \mu\text{m}$ for 8M100, the peak shifted to 0.216, 0.180, and $0.150 \mu\text{m}$ respectively for 8M75, 8M50 and 8M25. When considering the 10M, the structure of the pore network changed a little with more fine pores and an increase in connectivity that is justified with the appearance of a large spectra of pores with different size in the range 0.01 and $10 \mu\text{m}$. Increasing the concentration of NaOH to 12M, the capillary pores with size $\geq 0.24 \mu\text{m}$ decreased again and the porosity of the specimens saw their size shifted to smaller values: the volume of the fine pores increased while their size shifted with the increase of the standard sodium silicate solution. This is indicative of the difference in the structure of the two solutions even though they present similitudes in chemical composition, XRD and FT-IR spectroscopy. However the porosity and the pore size distribution achieved with RHA-NaOH solution in the range 8-12M are in agreement with the results available into the literature (Kamseu et al., 2014; Kamseu et al., 2013; Okada et al., 2011) and allow to defend RHA-NaOH solution as promising candidate for the design of low porous MK-Geopolymers. The specimens

with 100% of RHA-NaOH remain with relatively high values of water absorption (Fig. 7): between 13 and 14%. This can be explained essentially by the extend of dissolution of RHA in the solution. When considering NaOH 8M, RHA-NaOH demonstrated low solubility with respect to 10M and 12M. This low solubility conducted to the formation of more clusters and larger particles that are responsible for the microstructure coarsening with poor level of polymerization/polycondensation, reduction of the cross-linking with more capillary porosity that remains into the matrix (Fig. 3, 5 and 6). The reinforcement of RHA-NaOH with standard sodium silica as from 25% has as effects the reduction of the water absorption as the result of the reduction of the open porosity. As already indicated this reduction is also effective when the concentration of the initial NaOH increases. The increase of the pH of NaOH solution increases the formation of more Q^2 capable to induce more chemical linkages. This explain the similar effects with the presence of the standard sodium silicate into the formulations.

Fig. 8 shows the residual moisture into the samples of geopolymers after complete curing to constant weight at room temperature (> 90 days in this case at $21 \pm 2^\circ\text{C}$). Apart from the sample made with 100% of RHA-NaOH sodium silicate 8M, all specimens have the values of moisture between 6.5 and 7.9%. Values are in agreement with those available into the literature (Kamseu et al., 2012). The moisture content is easily correlated to the fraction of the fine pores present into the specimens. The general rule in the cases of the samples under study is that the extend of the dissolution (from 8M to 12M) or the fraction of the standard sodium silicate (25 to 75%) favors the formation of more fine pores that enhance the volume of moisture into the final matrix.

4.4 Densification, mechanical strength and microstructure

The flexural strength is in general appropriate for the evaluation of the extend of links and cross-linkings developed into the geopolymer matrices. This flexural strength expresses also the level of densification and it is the result of the microstructural features within the matrix of geopolymers (Fig. 9). Fig. 10 shows the bulk density and the mechanical strength of the different formulations of geopolymers as function of RHA/NaOH content and the pH value of the initial NaOH solution. The bulk density decreases with the increase of the fraction of RHA-NaOH based sodium silicate from 1.75 g.cm^{-3} at 25% to 1.5 g.cm^{-3} at 100%. The use of 100% of RHA-NaOH sodium silicate solution brings a significant difference in densification compared to the samples in which RHA-NaOH is partially replaced with the conventional sodium silicate solution (Fig 9). Independently on the concentration of the initial NaOH solution, the density of the formulations are stable between 50 and 75% of RHA-NaOH silicate solution. In fact as from 25% of standard silicate solution, it is observed that all the formulations presented values of density in the interval of that generally

observed into the literature (Kamseu et al., 2013, Kamseu et al., 2014, Kamseu et al., 2015). The increase of the alkalinity contribute to improve the dissolution and the polycondensation with the formation of more dense final products. These observations are in agreement with the hypothesis that between 8 and 12M of NaOH, the increase of the concentration of the initial alkaline solution contributes to the increase in dissolution and formation of more soluble silica oligomers capable to enhance the geopolymerization. These results of the densification are in line with the variation of the flexural strength (Fig 9 and 10). The use of 100% of RHA-NaOH sodium silicate solution conducts to final geopolymer composites with the flexural strength of 4 MPa at 8M of NaOH and 4.5 MPa at 12M of NaOH. With the partial replacement of standard sodium silicate by RHA-NaOH one, the flexural strength increased to 5 MPa at 25% of RHA-NaOH sodium silicate, and 6 MPa at 50% of RHA-NaOH sodium silicate. The flexural strength even reached 8 MPa with 75% of RHA-NaOH sodium silicate demonstrating that the combination of both types of sodium silicate is positive for the final properties of geopolymer composites. This is due to the fact that standard sodium silicate contains more fine molecular silica aggregates in solution while RHA-NaOH sodium silicate would have more coarse molecular compounds which when in specific percentage contribute to the formation of more dense and compact structure with high strength.

The micrographs of the specimens with 100% of RHA-NaOH sodium silicate solution show progressive improvement of the densification with the increase in concentration of the initial NaOH solution from 8 to 12M (Fig. 11). This can be easily correlated to the results of the bulk density and flexural strength (Fig. 9 and 10). The level of reactivity and densification is linked to the degree of dissolution and polycondensation: dissolution and polycondensation that is improved in the case of amorphous silica with the concentration of the alkaline solution. The microstructure of those specimens goes from coarser and porous at 8M (Fig. 11a) to more fine and dense matrix at 10M and 12M series (Fig. 11b and c). The specimens of the formulations with 10 and 12M are those with matrices similar to that of standard metakaolin based inorganic polymers. In the micrograph of geopolymers with initial NaOH solution of 8M, it can be observed a significant amount of metakaolin (still having the kaolin structure) that has not been affected during the geopolymerisation. This unreacted fraction of metakaolin coexist with residual non-dissolved amorphous RHA contributing to the poor densification of those matrices with 8M NaOH. The nanometric structure of polysialates (H-N-A-S) that can be observed in the Fig. 11c is typical of that of metakaolin based geopolymer matrix (Gao et al., 2014; Mo et al., 2014; Pelisser et al., 2013). It appeared that when the RHA is well dissolved into NaOH solution (cases of 10M and 12M), soluble silica is formed capable to play similar role as that of standard sodium silicate. The residues of alkalis observed into XRD and FT-IR patterns of specimens with high concentration of NaOH seem

not to affect the final product. However, it should be noted that the production of the standard sodium silicate include a final stage of filtration and neutralization which affect the final cost of the solution. Those two steps in the case of the use of RHA-NaOH based sodium silicate solution for the production of geopolymers have to be avoided since residues of alkalis and that of amorphous silica can be managed using the mix-design. In our investigations, it was clearly observed that the effects of the residual alkalis into the solidified sodium silicate solution with the sodium carbonates formed are influenced by the initial concentration of NaOH used. However the presence of carbonates into the matrices of geopolymers was inversely proportional to the concentration of the initial NaOH. The higher the concentration of initial sodium silicate, the lower the carbonate concentration into the final geopolymer matrices (Fig. 12). This confirms the fact that the in situ preparation of the sodium silicate as from RHA can be well monitored with the mix-design to achieve optimal quality of the metakaolin based geopolymer composites. Fig. 10 shows the micrographs of the specimens produced with 50 to 75 vol.% of RHA-NaOH based sodium silicate solution. The presence of the components into the metakaolin and sand capable to fix unreacted elements from sodium silicate is contributive for the good compaction and adhesion bonds observed at high magnification (Fig. 13).

5. Discussion

Fawer et al. (2012) described four major commercial production routes for the sodium silicate. For the geopolymerization, sodium silicate with molar ratio between 2 and 3.3 are generally used (Davidovits, 2008; Kamseu et al., 2014; Kamseu et al., 2013; Kamseu et al., 2012; Okada et al., 2011). Sodium silicate with MR of 3.3 is produced by direct fusion of precisely measured proportions of pure silica sand and soda ash at temperature $\sim 1400^{\circ}\text{C}$. This class of sodium silicate has high cost and high Global Warming Potential (GWP). Its use in geopolymers will increase the rate of CO_2 emitted and influence the sustainability of the final product. Relatively low molar ratio (~ 2) of sodium silicate solution is produced by hydrothermal dissolution of silica in sodium hydroxide solution. This kind of sodium silicate with molar ratio 2 is described into the literature as having low GWP because of the low temperature required for their production. The furnace process accounts for 80-90% of the energy consumption in the cycle of the production of high molar ratio of sodium silicate (Fawer et al., 2012). Therefore, the GWP of sodium silicate produced at relatively low temperature can be reduced by 50-70% or more if we consider the Rice Husk Ash as source of amorphous silica and its calcination as waste treatment. RHA offers the advantage that it can be dissolved easily into high concentrated NaOH solution. The silicate oligomers that are formed are function of the concentration of NaOH and the extend of dissolution of RHA. Tchakouté et al.

(2016a and 2016b) proposed a pre-treatment of rice husk ash and waste glasses which increase the cost and affect the environmental impact of the final products. The solution of the present study appears as one of the more sustainable route for the substitution of the standard commercial sodium silicate solution into structural matrices of geopolymers.

Studying the Global Warming Potential of the components of geopolymer in details, Heath et al. (2014) indicated that sodium silicate accounts to 44-59% and being the major concern regarding the environmental impacts for the production of this new class of materials. Our approach works without the fusion into the furnace as well as filtering since the residual undissolved amorphous silica are going to remain into the matrix acting as filler or contributing in the interfacial reactions at the level of interfaces of grain particles of geopolymers.

From the phases evolution, mechanical strength and microstructure (Fig. 9, 11 and 13), it was concluded that the production of RHA-NaOH based sodium silicate solution with equilibrated fractions of monomers, clusters and larger colloidal particles is capable to achieve good densification and strength. The necessity of having this equilibrium between fractions of monomers, clusters and colloidal particles of sodium silicate solution suggested ideal composite solution made of ~ 25 vol.% of standard and up to 75 vol.% of RHA-NaOH based sodium silicate solution.

The hypothesis of using RHA-NaOH based sodium silicate, to replace partially up to 75 vol.% the standard sodium silicate, provide significant reductions in the GWP of metakaolin-based geopolymers. The mix-design in this context insure similar bulk composition and therefore the physico-mechanical performance can be monitored to present final matrix with optimum characteristics. The use of multiple precursors, activators and curing temperatures for geopolymer manufacturing can lead to complex mix design, but has the potential to reduce the GWP potential to a level well below that of “just add water” of Portland cement (Heath et al., 2014).

Conclusion

RHA-NaOH based sodium silicate solution cured at room temperature in open air showed characteristics (FT-IR and XRD) similar to that of standard sodium silicate solution of same bulk composition with $\text{SiO}_2/\text{Na}_2\text{O}$ molar ratio of 3.1. The presence of carbonates was evidenced in RHA-NaOH solidified sodium solution and increase in intensity with the increase of the initial concentration of NaOH. 100 vol.% of RHA-NaOH sodium silicate solution conducted to metakaolin based geopolymer with relatively high cumulative pore volume and more porous microstructure. From the phases analysis and microstructural investigations, the above described behavior were ascribed to the effectiveness of the dissolution of RHA and formation of different classes of silica oligomers as function of the initial NaOH concentration.

The association between standard sodium silicate and RHA-NaOH one contributed to the production of good matrix with optimum mechanical strength correlated to good densification. 25 vol.% of the standard sodium silicate seem sufficient to equilibrated 75 vol.% of RHA-NaOH sodium silicate solution with effective action as binder in metakaolin based geopolymer matrix. The mechanism of the improvement in densification and strength is found on the symbiotic effects between the Q^2 of the standard sodium silicate solution and the Q^3 and Q^4 of the RHA-NaOH sodium silicate solution.

The design of metakaolin based geopolymer composites with 75 vol.% of sodium silicate replaced with RHA-NaOH sodium silicate reduces the environmental impacts of the geopolymerization and appears as a viable solution for the production of sustainable geopolymers.

References

- Bignozzi, M.C., Manzi, S., Lancellotti, I., Kamseu, E., Barbieri, L., Leonelli, C., 2013. Mix-design and characterization of alkali activated materials based on metakaolin and ladle slag. *Appl. Clay Sci.* 73 (1), 78–85. doi:10.1016/j.clay.2012.09.015.
- Brew, D.R.M., Glasser, F.P., 2005. Synthesis and characterisation of magnesium silicate hydrate gels. *Cem. Concr. Res.* 35, 85–98.
- Chandrasekhar, S., Satyanarayana, K.G., Pramada, P.N., Raghavan, P., Gupta, T.N., 2003. Processing, properties and applications of reactive silica from rice husk ash - an overview. *J. Mater. Sci.* 38, 3159–3168.
- Davidovits, J., 2008. *Geopolymer chemistry and applications*. Publ. Morrisville, USA, p. 570.
- Fawer, M., Concannon, M., Reiber, W., 1999. Life cycle inventories for the production of sodium silicates. *Int J. LCA* 4 (4), 2007–2012.
- Gerschel, A., 1995. *Liaisons intermoléculaires: les forces en jeu dans la matière condensée*. Savoir Actuels. p. 274 <http://www.amazon.fr/dp/2729603743>.
- Habert, G., D'Espinose De Lacaillerie J.B., Roussel, N., 2011. An environmental evaluation of geopolymer based concrete production: reviewing current research trends. *J. Clean. Prod.* 19 (11), 1229–1238. doi:10.1016/j.jclepro.2011.03.012.
- Heath, A., Paine, K., McManus, M., 2014. Minimising the Global Warming Potential of clay based geopolymers. *J. Clean. Prod.* 78: 75–83. doi:10.1016/j.jclepro.2014.04.046.
- Kamseu, E., Bignozzi M., Melo, U.C., Leonelli, C., Sglavo, V., 2013. Design of inorganic polymer cements: effects of matrix strengthening on microstructure. *Constr. Build. Mater.* 38, 1135–1145. doi:10.1016/j.conbuildmat.2012.09.033.

- Kamseu, E., Nait-Ali, B., Bignozzi, M.C., Leonelli, C., Rossignol, S., Smith, D.S., 2012. Bulk composition and microstructure dependence of effective thermal conductivity of porous inorganic Polymer Cements. *J. Eur. Ceram. Soc.* 32 (8), 1593–1603. doi:10.1016/j.jeurceramsoc.2011.12.030.
- Kamseu, E., Cannio, M., Obonyo, E., Tobias, F., Chiara, M., Sglavo, V., Leonelli, C., 2014. Cement & concrete composites metakaolin-based inorganic polymer composite : effects of fine aggregate composition and structure on porosity evolution, microstructure and mechanical properties. *Cem. Concr. Compos.* 53, 258–269. doi:10.1016/j.cemconcomp.2014.07.008.
- Kang Gao, Kae-Long Lin, DeYing Wang, Chao-Lung Hwang, Hau-Shing Shiu, Yu-Min Chang, Ta-Wui Cheng, 2014. Effects SiO₂/Na₂O molar ratio on mechanical properties and the microstructure of nano-sio₂ metakaolin-based geopolymers. *Constr. Build. Mater.* 53, 503–510.
- McLellan, B.C., Williams, R.P., Lay, J., van Riessen, A., Corder, G.D., 2011. Costs and carbon emissions for geopolymer pastes in comparison to ordinary portland cement. *J. Clean. Prod.* 19, 1080–1090.
- Mehta, P.K., 1973. Siliceous ashes and hydraulic cements prepared therefrom. Belgium Patent 802909.
- Mehta, P.K., 1992. Rice husk ash – a unique supplementary cement material. In Edited: Malhotra, V.M. *Proceeding of International Conference on Advance in Concrete Technology – CANMET*. Greece, pp. 407–31.
- Mo, Bing-hui, Zhu, He, Cui, Xue-min, He, Yan, Gong, Si-yu, 2014. Effect of curing temperature on geopolymerization of metakaolin-based geopolymers. *Appl. Clay Sci.* 99, 144–48.
- Nagrle, S.D., Dr. Hajare Hemant, Modak Pankaj, R., 2012. Utilization of rice husk ash. *Int. J. Eng. Res. Appl.* 2, 1–5.
- Nordstrom A., Sundblom, A., Jensen, G.V., Pedersen, J.S., Palmqvist, A., Matic, A., 2013. Silica/alkali ratio dependence of the microscopic structure of sodium silicate solutions. *J. Colloid Interface Sci.* 397, 9–17. doi:10.1016/j.jcis.2013.01.048.
- Nordstrom, J., Nilsson, E., Jarvol, P., Moheb Nayeri, Palmqvist, A., Bergenholtz, J., Matic, A., 2011. “Concentration-and pH-Dependence of Higly Alkaline Sodium Silicate Solutions.” *J. Colloid Surf. Sci.* 356, 37–45.
- Okada, K., Imase, A., Isobe, T., Nakajima, A., 2011. Capillary rise properties of porous geopolymers prepared by an extrusion method using polylactic acid (PLA) fibers as the pore formers. *J. Eur. Ceram. Soc.* 31 (4), 461–67.
- Pelisser, F., Guerrino, E.L., Menger, M., Michel, M.D., Labrincha, J.A., 2013. Micromechanical Characterization of Metakaolin-Based Geopolymers. *Constr. Build. Mater.* 49, 547–53. doi:10.1016/j.conbuildmat.2013.08.081.
- Rodriguez, E.D., Bernal, S.A., Provis, J.L., Paya, J., Monzo, J.M., Borrachero, M.V., 2013. Effect of Nanosilica -Based Activators on the Performance of an Alkali-Activated Fly Ash Binder.” *Cem. Concr. Compos.* 35 (1), 1–11. doi:10.1016/j.cemconcomp.2012.08.025.

- Svensson, I.L., Sjöberg, S., Ohman, L.-O., 1986. Polysilicate equilibria in concentrated sodium silicate solutions. *J. Chem. Soc., Faraday Trans.* 82 (1), 3635–3646.
- Tchakouté, H.K., Rüschler, C.H., Kong, S., Ranjbar, N., 2016. Synthesis of sodium waterglass from white rice husk ash as an activator to produce metakaolin-based geopolymer cements. *J. Build. Eng.* 6, 252–261.
- Tchakouté, H.K., Rüschler, C.H., Kong, S., Kamseu, E., Leonelli, C., 2016. Geopolymer binders from metakaolin using sodium waterglass from waste glass and rice husk ash as alternative activators: A comparative study. *Constr. Build. Mater.* 114, 276–289. doi: 10.1016/j.conbuildmat.2016.03.184
- Tognonvi, M.T., Soro, J., Gelet, J.L., Rossignol, S., 2012. Physico-chemistry of silica/Na silicate interactions during consolidation. Part 2: effect of pH. *J. Non. Cryst. Solids* 358 (3): 492–501.
- Tognonvi, M.T., Soro, J., Rossignol, S., 2012. Physical-chemistry of silica/alkaline silicate interactions during consolidation. Part 1: effect of cation size. *J. Non. Cryst. Solids* 358 (1), 81–87.
- Turner, L.K., Collins, F.G., 2013. Carbon dioxide equivalent (CO₂-E) emissions: a comparison between geopolymer and OPC cement concrete. *Constr. Build. Mater.* 43, 125–130.
- White, C.E., Provis, J.L., Llobet, A.L., Proffen, T., van Deventer, J.S.J., 2011. Evolution of Local Structure in Geopolymer Gels: An in Situ Neutron Pair Distribution Function Analysis. *J. Am. Ceram. Soc.* 94 (10), 3353–3532.

Figures and Tables Captions

Figure 1: XRD patterns of the standard and RHA-NaOH based sodium silicate solutions showing the impact of NaOH concentration into the formation of silicate oligomers.

Figure 2: FT-IR spectroscopy patterns of the standard and RHA-NaOH based sodium silicate solutions showing the impact of NaOH concentration into the formation of silicate oligomers.

Figure 3: FT-IR spectroscopy patterns of geopolymers as function of the RHA-NaOH sodium silicate content.

Figure 4: XRD patterns of geopolymers as function of the RHA-NaOH sodium silicate content.

Figure 5: Cumulative pore volume of metakaolin based geopolymers as function of the RHA-NaOH sodium silicate solution.

Figure 6: Pore size distribution of metakaolin based geopolymers as function of the RHA-NaOH sodium silicate solution.

Figure 7: Water Absorption of metakaolin based geopolymers as function of the RHA-NaOH sodium silicate solution.

Figure 8: Variation of the moisture content as function of the molarity of the concentration of the initial NaOH solution.

Figure 9: Flexural strength of metakaolin based geopolymers as function of the RHA-NaOH sodium silicate solution.

Figure 10: Variation of the Bulk density (g.cm^{-3}) of metakaolin based geopolymers as function of the RHA-NaOH sodium silicate solution.

Figure 11: Micrographs of metakaolin based geopolymers: (a) 8M100; (b) 10M100; (c) 12M100.

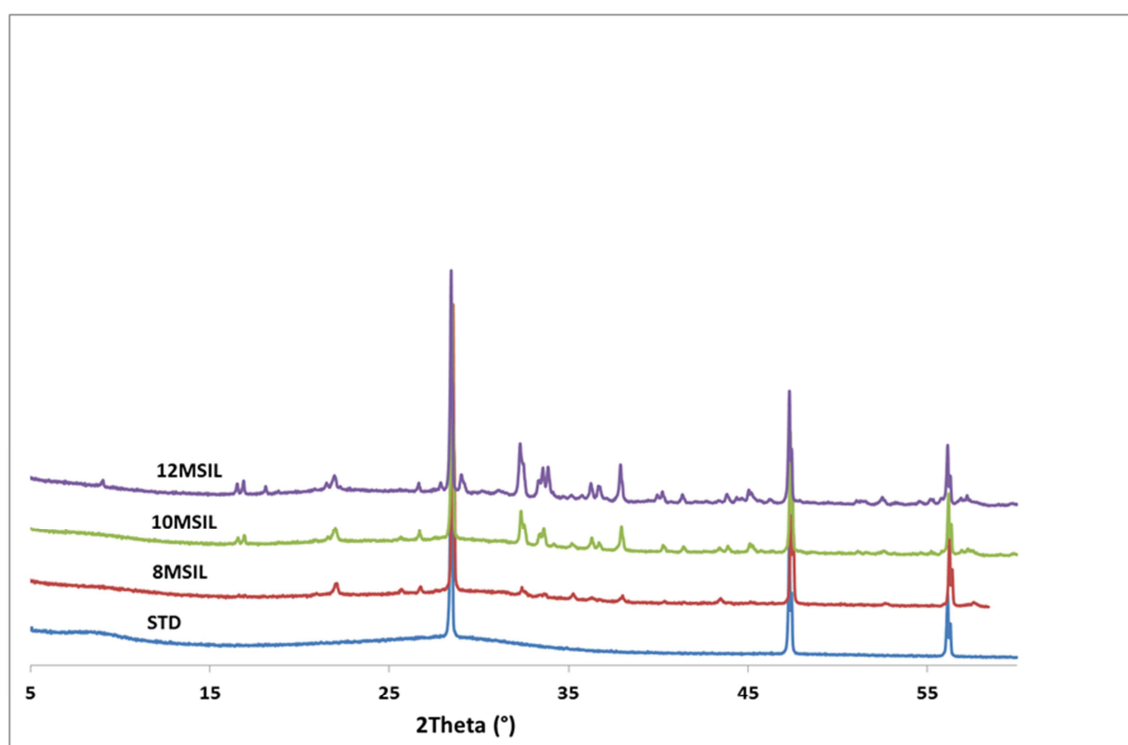
Figure 12: Variation of the carbonates content into the final matrices of metakaolin based geopolymers as function of RHA-NaOH sodium silicate content.

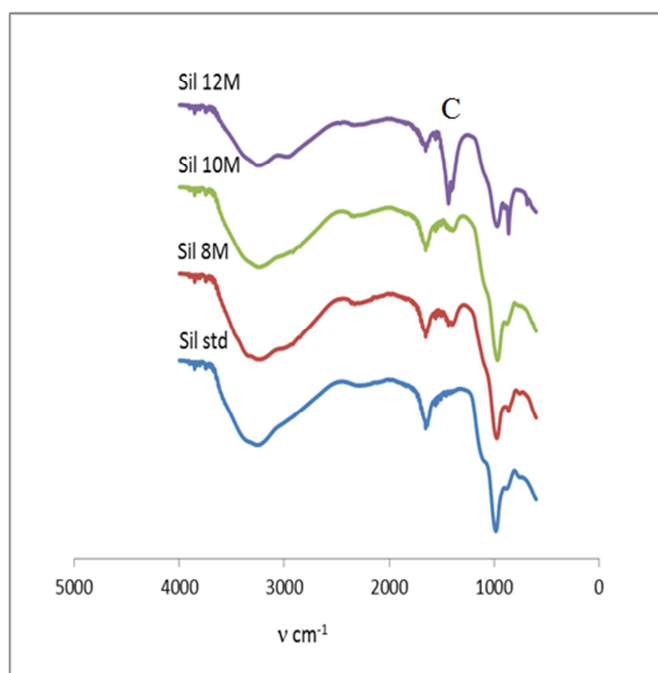
Figure 13: Micrographs of high compact matrix made of 25 vol.% of standard commercial sodium silicate and 75 vol.% RHA-NaOH silicate.

Table 1: Physical properties of the metakaolin and RHA used for the formulation of geopolymer composites.

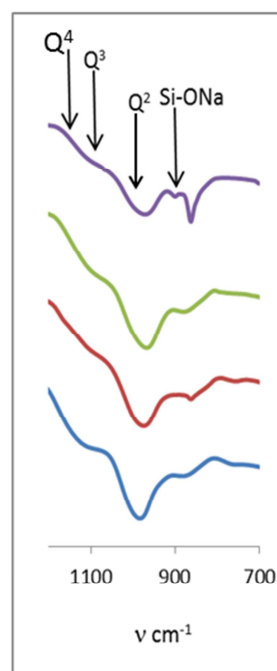
Table 1: Physical properties of the metakaolin and RHA used for the formulation of geopolymer composites.

Materials	Physico-chemical properties			
	Bulk composition	Specific area g/cm^2	Specific density $\text{g}.\text{cm}^{-3}$	Particles under $10\text{ }\mu\text{m}$
Metakaolin	$5.4\text{SiO}_2.4\text{Al}_2\text{O}_3$	37	1.23	74.8
RHA	SiO_2	42	2.21	100
River Sand	SiO_2	/	2.34	1.2

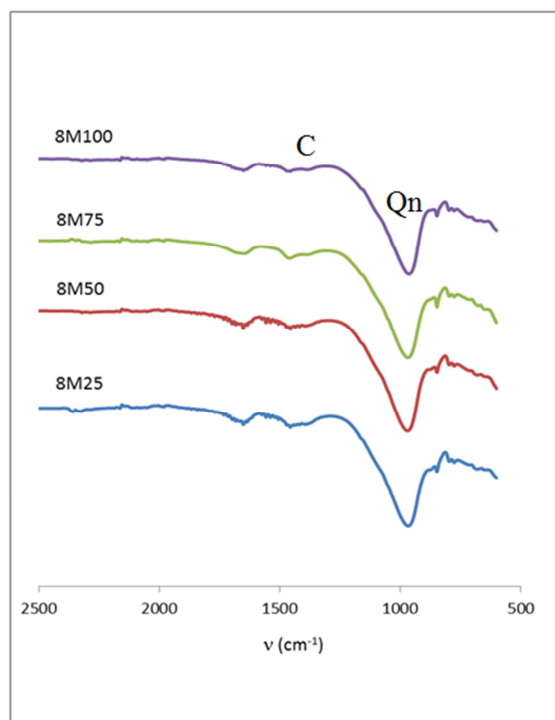


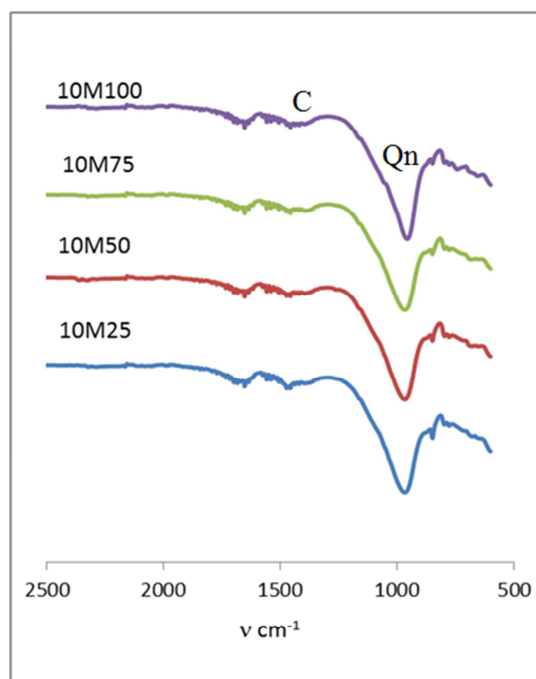


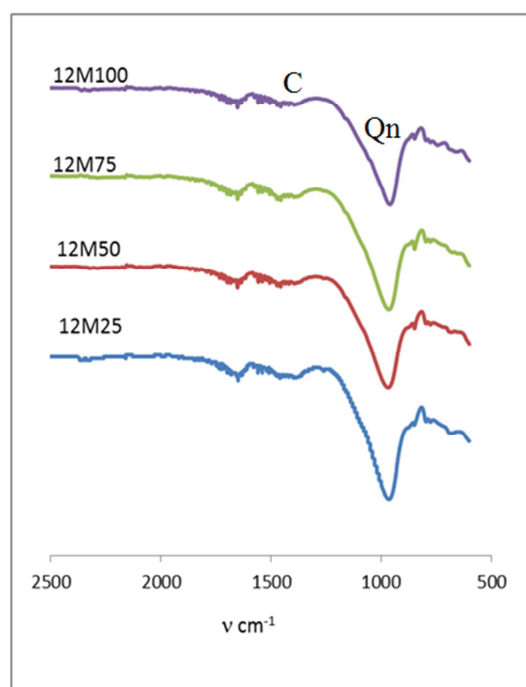
a

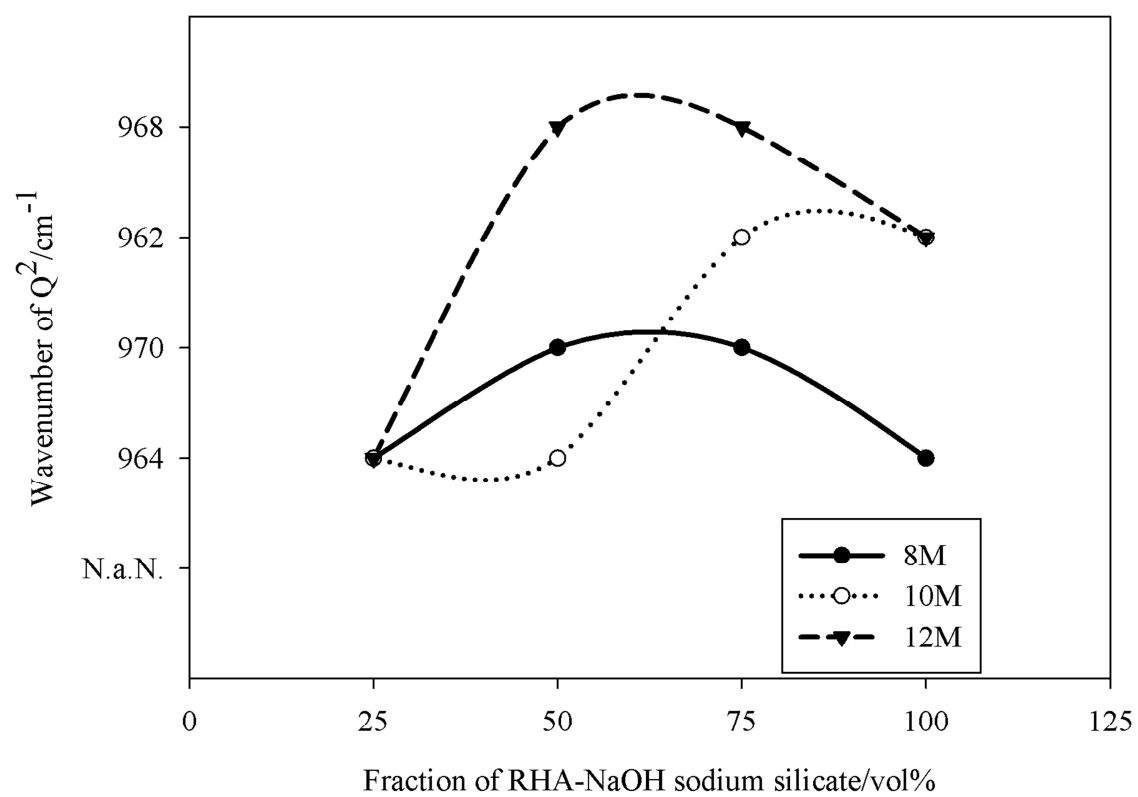


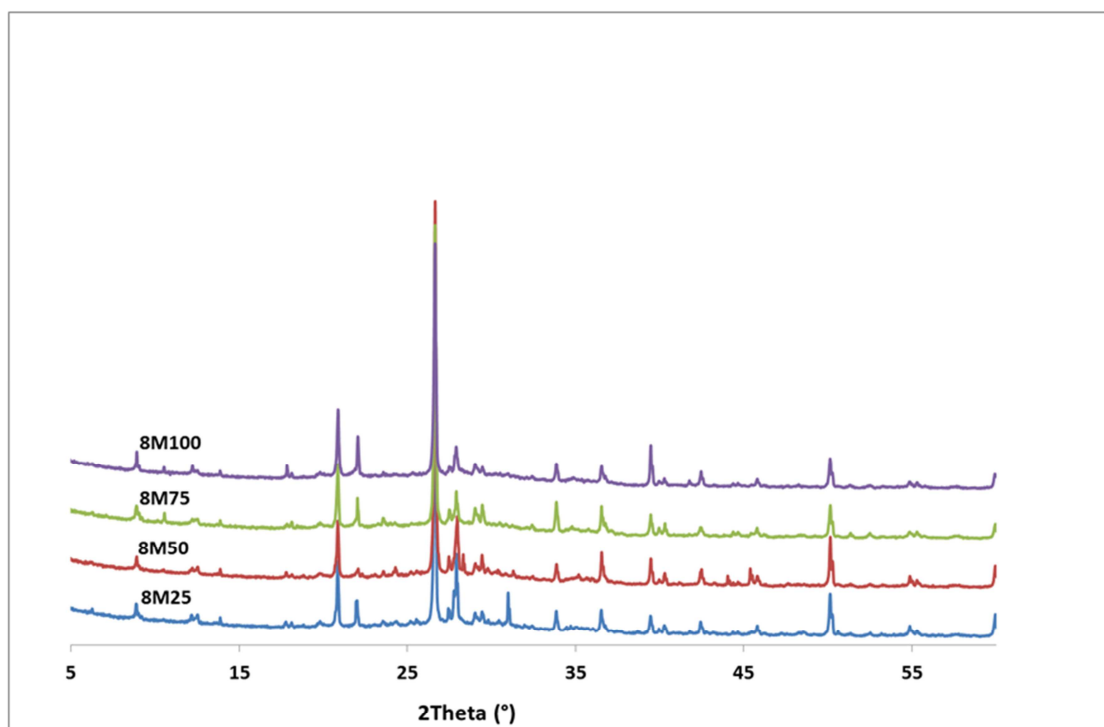
b

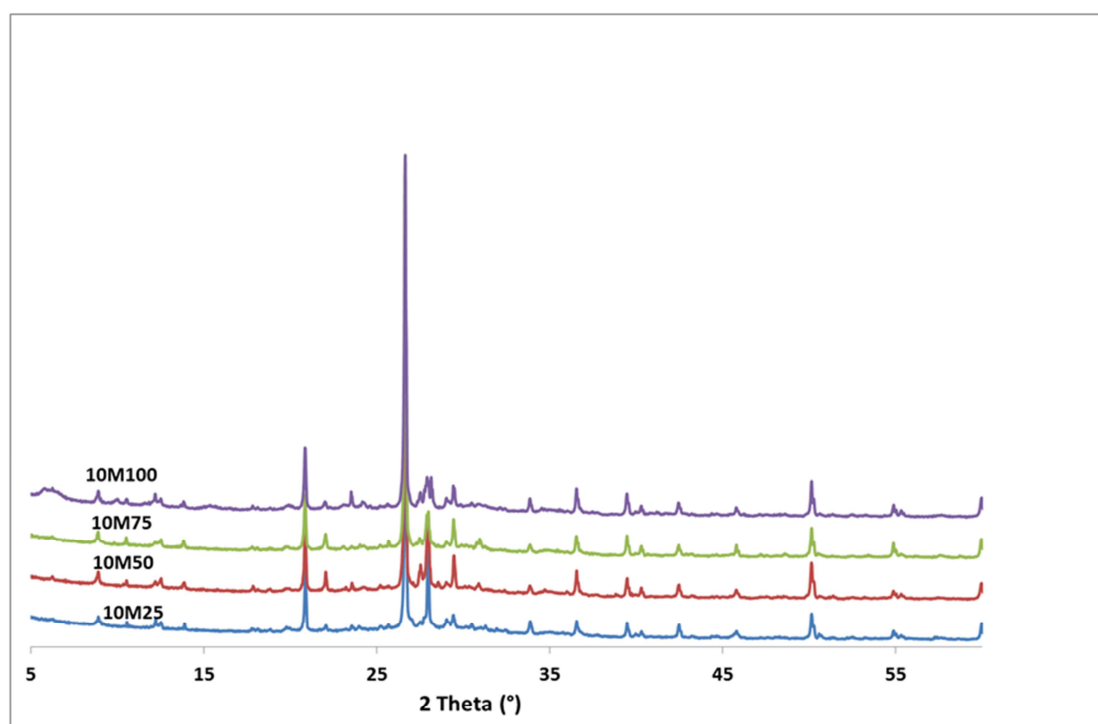


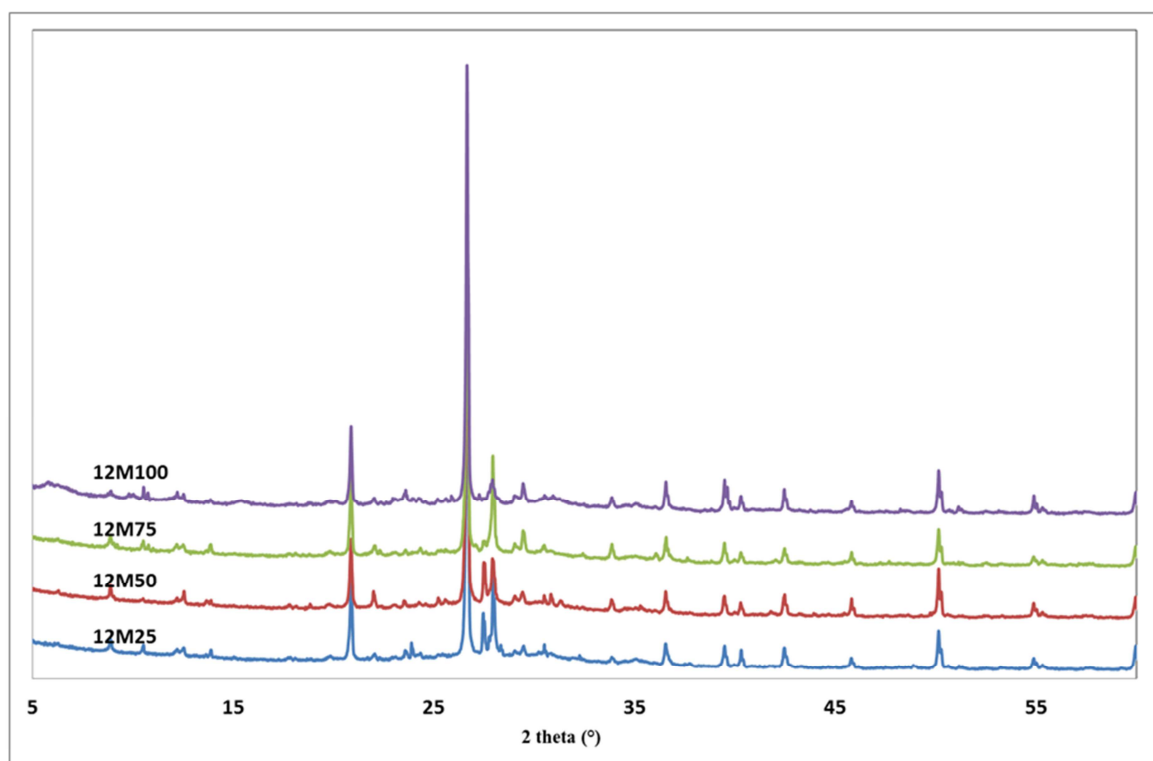


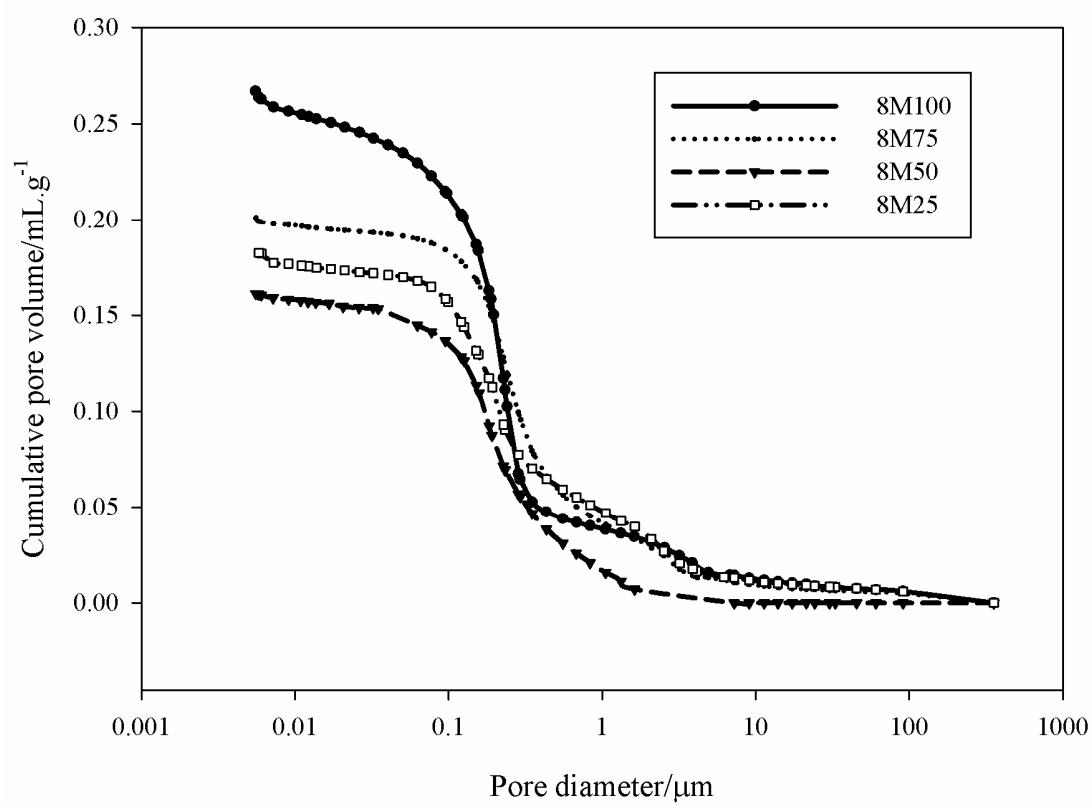


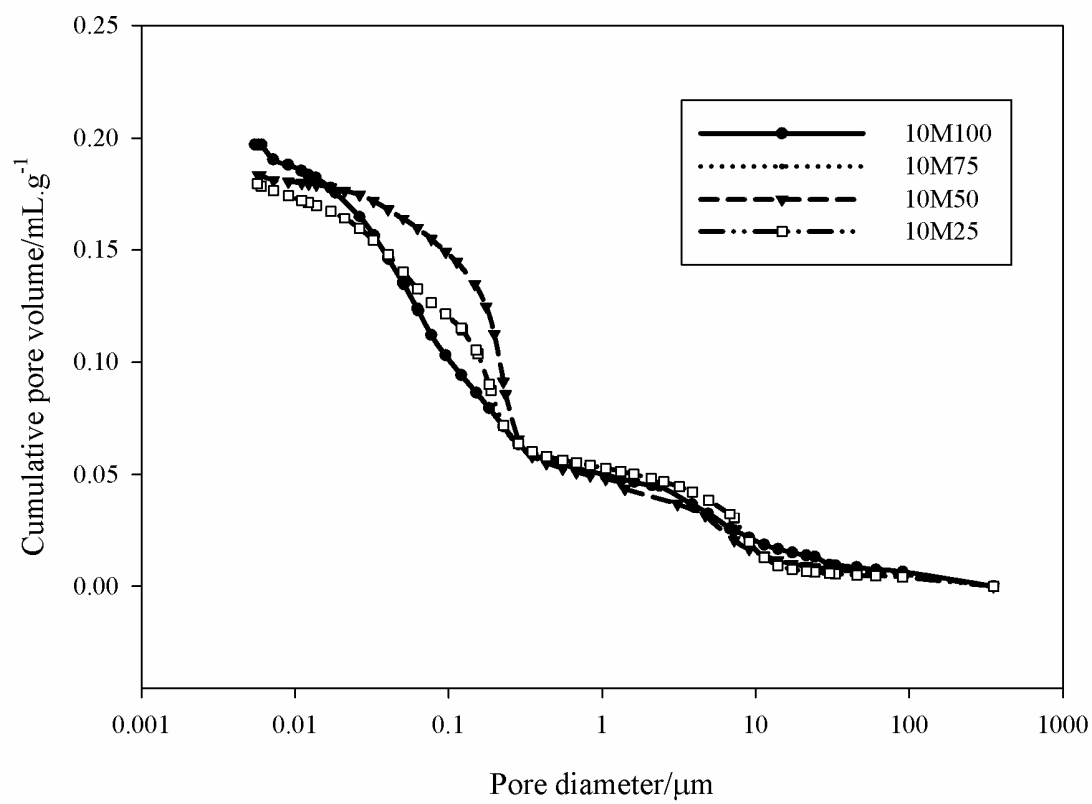


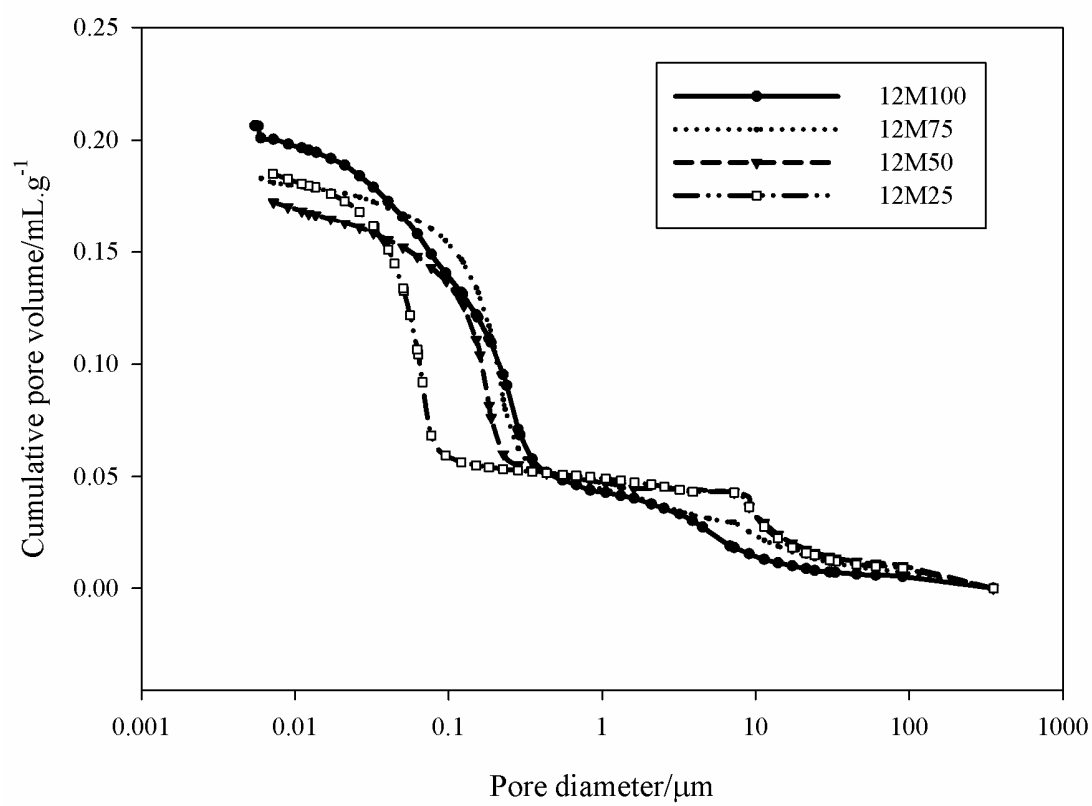


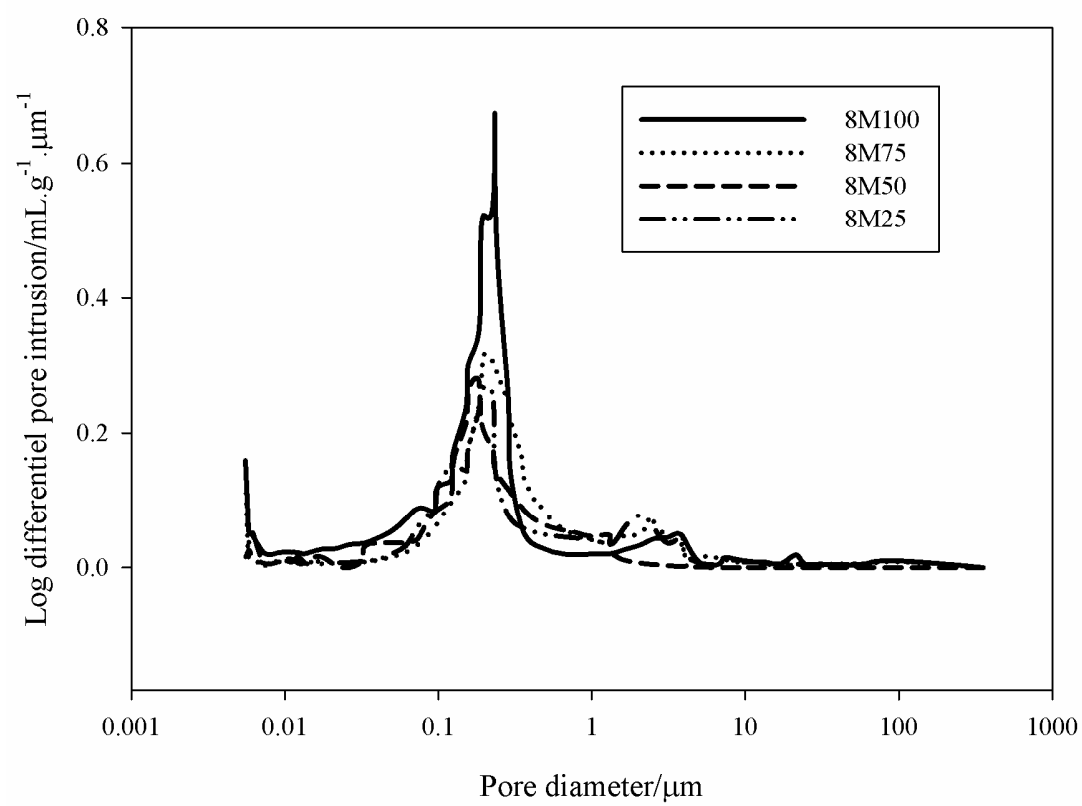


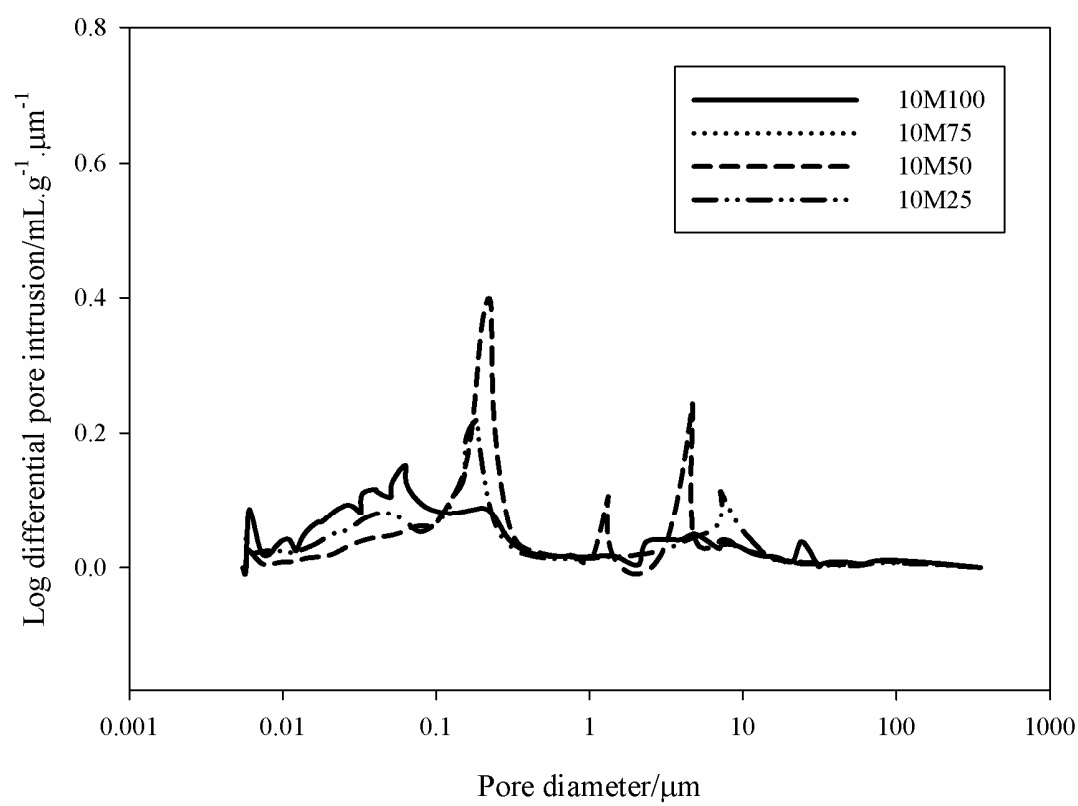


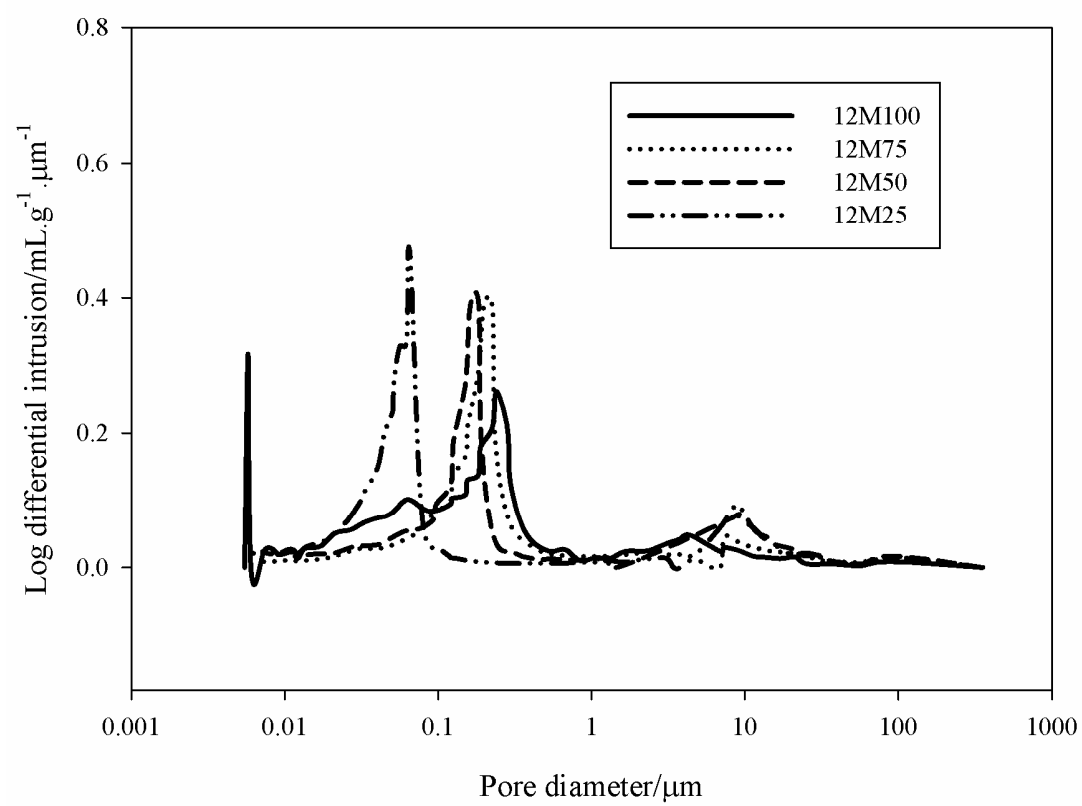


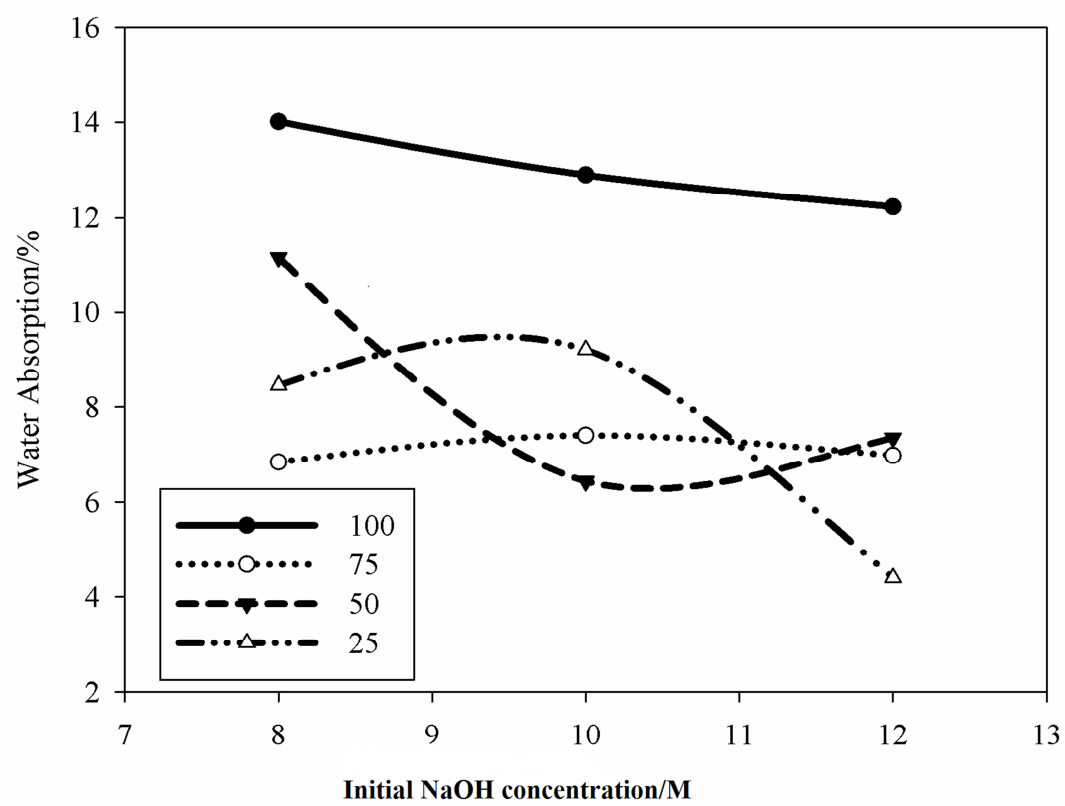


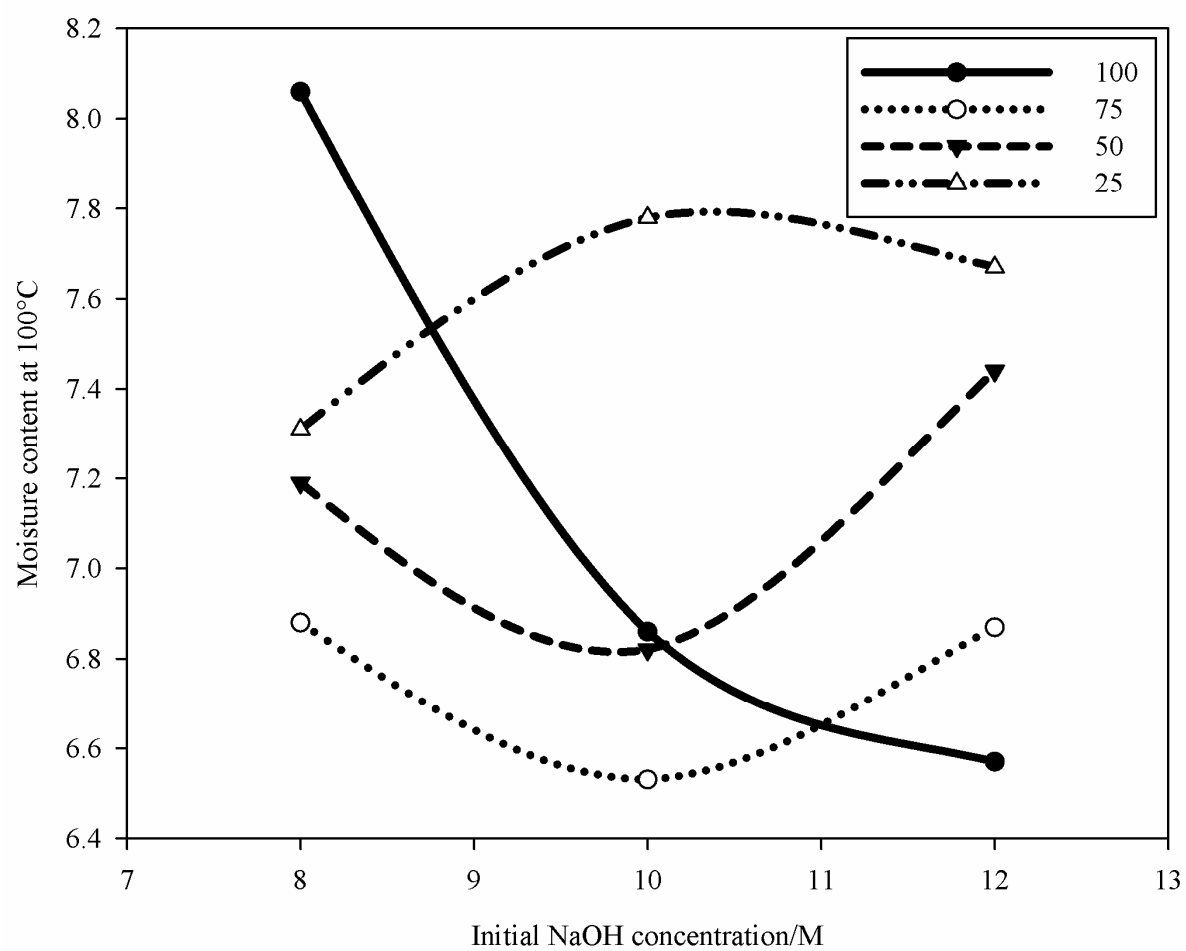


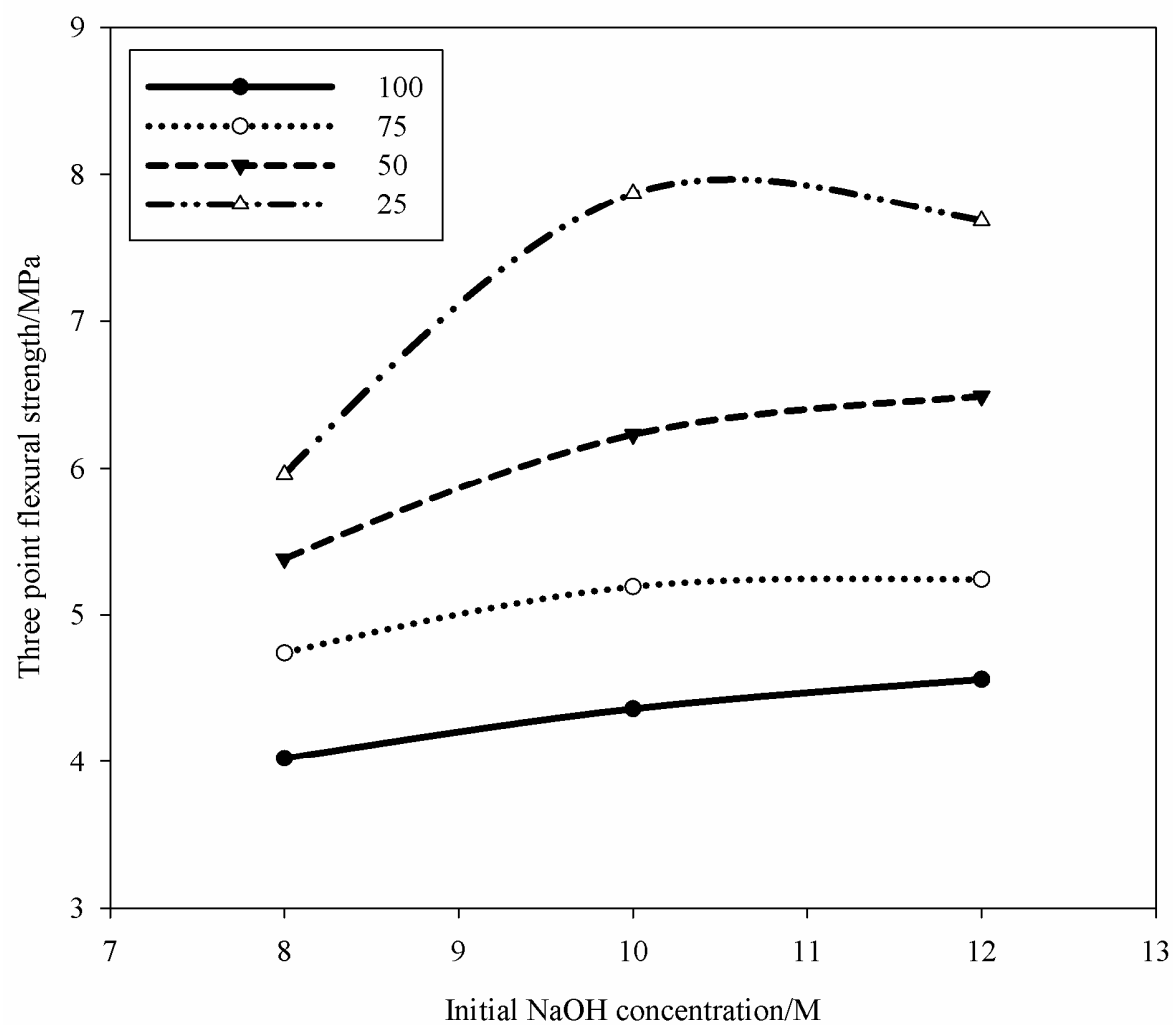


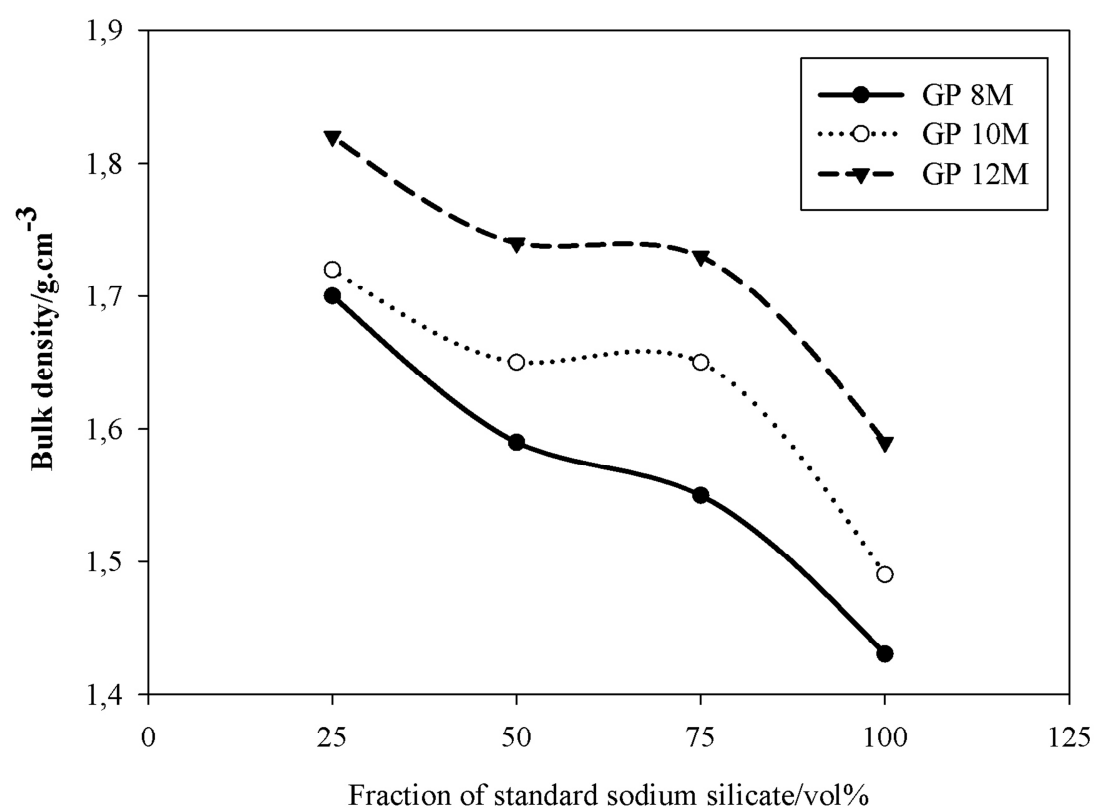


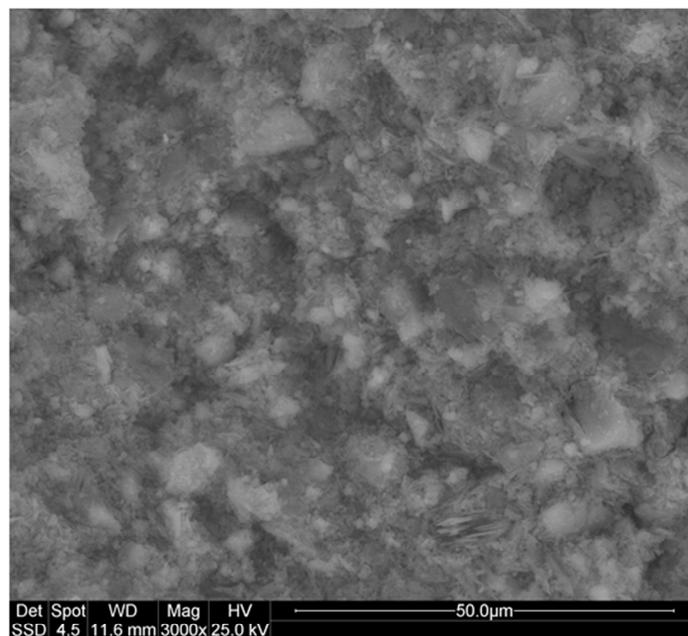






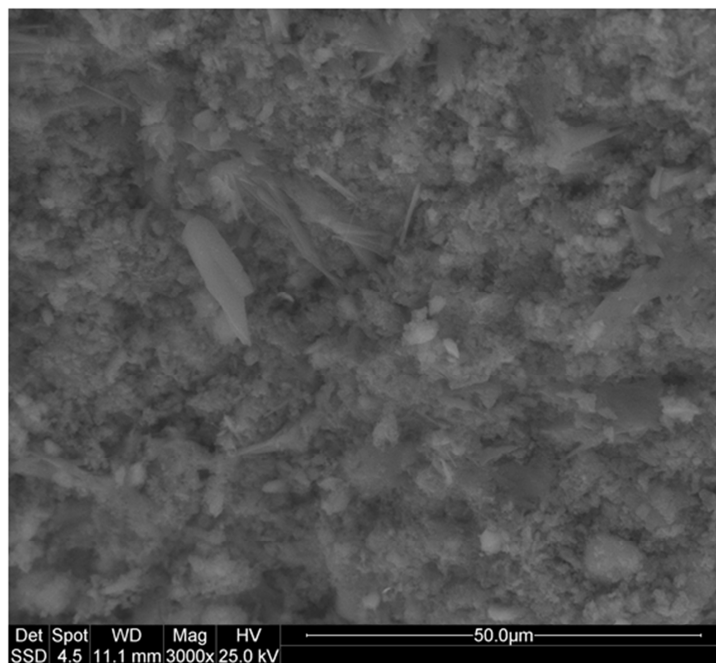




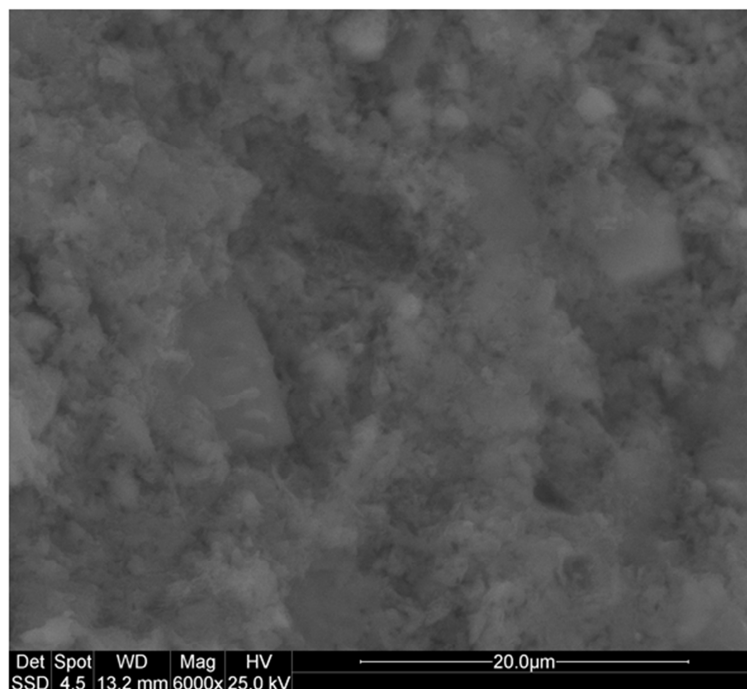


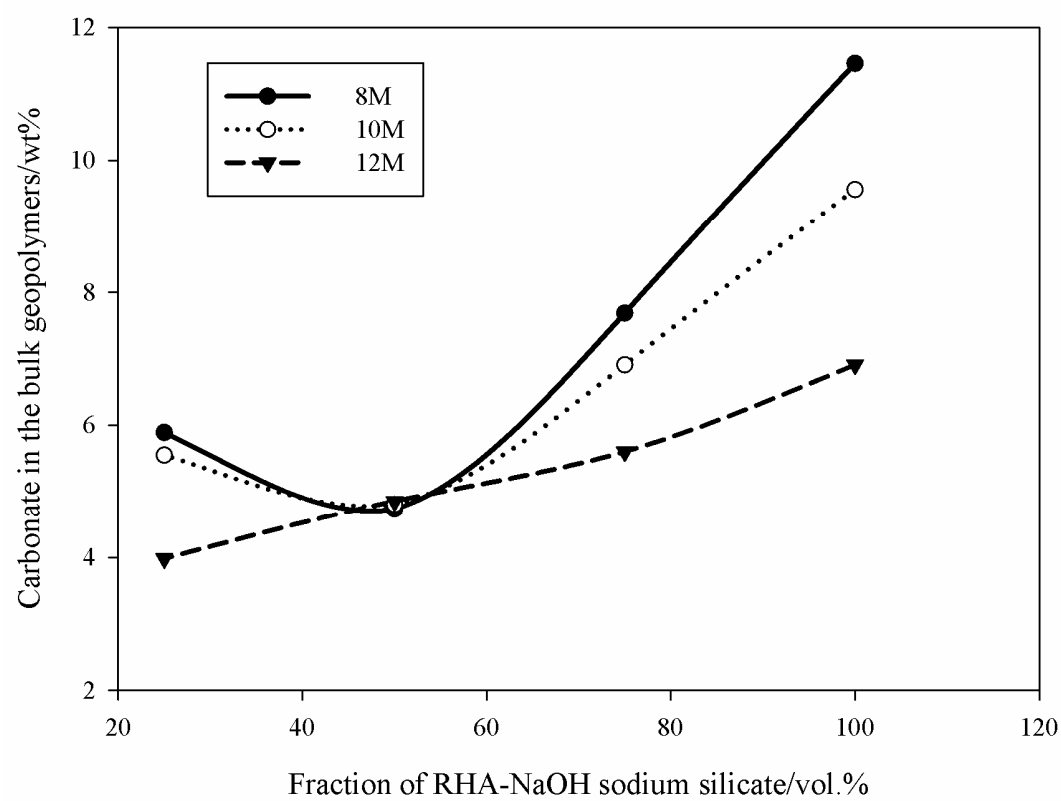
a

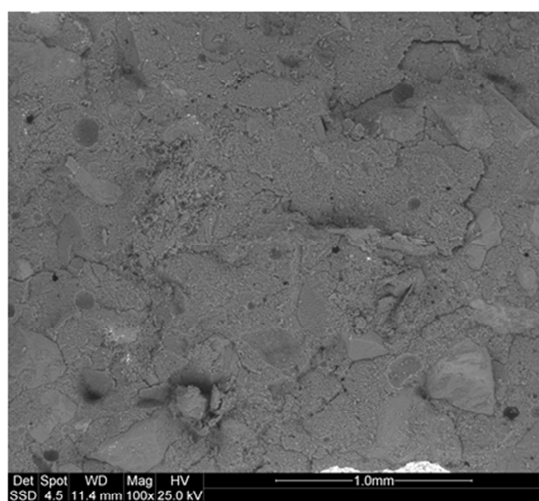
ACCEPTED



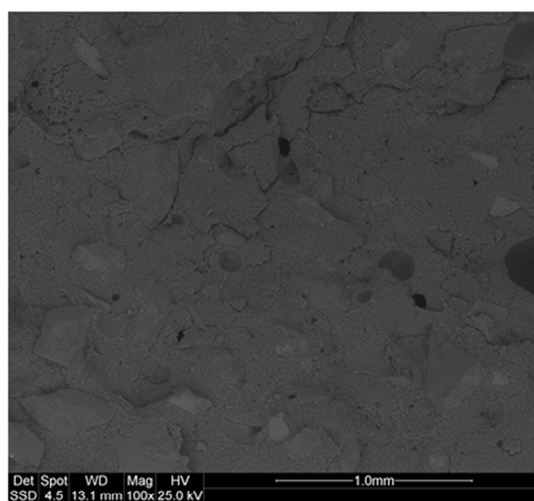
ACCEPTED





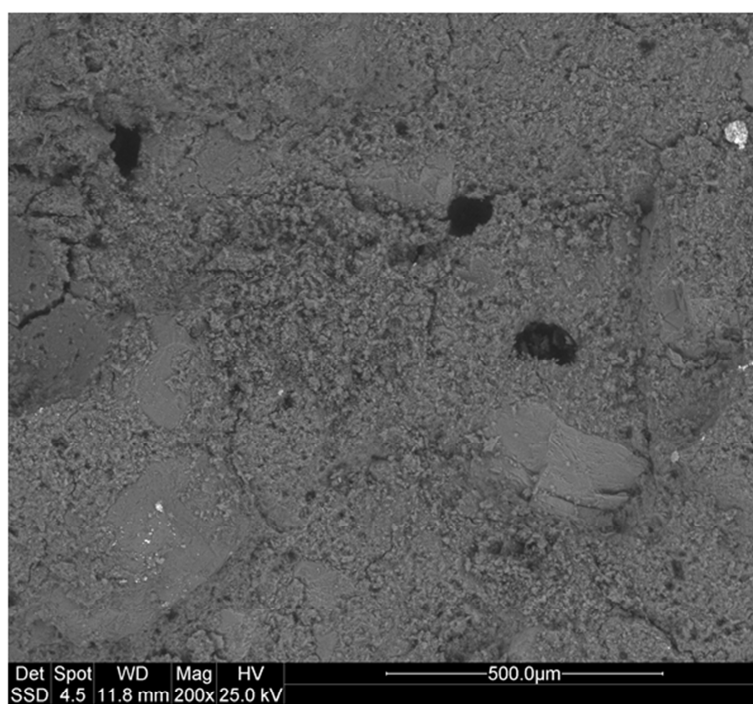


a



b

ACCEPTED



ACCEPTED

Highlights

- RHA-NaOH sodium silicate have similar characteristics to that of standard one.
- 75 vol.% of standard sodium silicate replaced with RHA-NaOH as a sustainable binder
- Using RHA-NaOH sodium silicates for geopolymers manufacture reduce the GWP